Electron-induced CCl_4 Adsorption on Ice

by

Hanwen Liu

A thesis

presented to the University of Waterloo

in fulfillment of the

thesis requirement for the degree of

Master of Science

in

Physics

Waterloo, Ontario, Canada, 2012

Author's Declaration

I hereby declare that I am the sole author of this thesis. This is a true copy of the thesis, including any required final revisions, as accepted by my examiners.

I understand that my thesis may be made electronically available to the public.

Abstract

Charge-induced adsorption is a subject of significance to environmental and biological systems. Ice surface is believed to get charged with potassium deposition. Compared to uncharged ice film, the work function of charged ice film is significantly reduced due to the formation of metastable delocalized excess surface electrons donated by potassium atoms on ice. This charging effect is found to be dependent on temperature. It is also reported that adsorption of CCl_4 would occur drastically on charged ice surface while almost no adsorption was observed on uncharged ice surface at low temperature. In addition, the results strongly agree with the cosmic-ray-driven electron-induced reaction (CRE) model for ozone depletion.

Acknowledgements

I’m extremely grateful to my supervisor Prof. Qing-Bin Lu for his kind guidance and support during the past two years. I also would like to thank Prof. Russell Thompson and Prof. Anton Burkov for their time and comments. Many thanks go to all the other members of Prof. Lu’s laboratory and my friends, for their support and friendship.

To My Parents

Table of Contents

List of Figures

List of Tables

Chapter 1

Introduction

Adsorption can be found in many physical, chemical, and biological systems in nature and varieties of applications in industry. It happens when interactions between particles and a surface are strong enough to make the particles stick to the surface. In this project, we focused on electron-induced adsorption. Therefore, the adsorption process was affected by charged surface. Indeed, charge-induced adsorption is involved in many environmental, geological, atmospheric and biological systems. In particular, charge-induced adsorption may play an important role in the cosmic-ray-driven electron-induced reaction (CRE) model for ozone depletion.[1] More details of this model can be found in section 1.2.2. Taking tetrachloride (CCl_4) as an example for ozone-depleting halogen-containing molecules, we study the possible adsorption process of CCl_4 on uncharged and charged ice surfaces, which is closely relevant to the CRE model for ozone depletion.

Field-induced adsorption, which is similar to charge-induced adsorption, has been observed and studied since the invention of field ion microscopy. Imaging gas, such as helium or neon, is observed to be adsorbed on the metal tip with the presence of electric fields.[2,3,4] Field-induced chemisorption was proposed by H. J. Kreuzer et al. to explain this phenomenon.[5,6] In 1998, H. M. van Driel et al. reported a universal mechanism for gas adsorption and electron trapping on oxidized silicon, in which charged surface creates the possibility for field-induced chemisorption of gases.[7] This will be discussed in details in section 1.3.

In this chapter, two main models for ozone depletion are first introduced in Section 1.1. Then a brief review of electron involved adsorption and desorption is presented in Section 1.2. Finally, the essential knowledge of electron-induced adsorption on ice surface regarding to this project will be discussed in Section 1.3, 1.4, and 1.5.

1.1. Models for ozone depletion

The ozone layer is well known because it can absorb ultraviolet (UV) rays. The UV generated by the sun can cause sunburn or skin cancer in human as well as DNA damage in living tissues of animals and plants. Life on Earth would not survive without the ozone layer. Unfortunately, ozone depletion has become one of the major environmental problems for the whole world today. Thus, stopping ozone depletion is a big challenge we have to face for the survival of all living things on earth. As we know, chlorofluorocarbons (CFCs), which are commonly known as Freons, have been recognized as the major ozone depleting molecules. Intensive research works studying CFCs have been carried out to explain the mechanism of ozone depletion. In general, chlorine atoms are regarded as the culprits for ozone depletion by the following reaction cycle.

$$Cl + O_3 \rightarrow ClO + O_2 \qquad (1\text{-}1)$$

$$ClO + O \rightarrow Cl + O_2 \qquad (1\text{-}2)$$

However, there are two main different models for the depletion of ozone, the photochemical model and the cosmic-ray-driven electron reaction model, which give different pathways for the production of chlorine atom. Details are discussed below.

1.1.1. The photochemical model

This model was first proposed by Molina and Rowland in 1974. They found the chlorine atoms can be produced from CFCs by sunlight photolysis[8]:

$$CF_2Cl_2 + h\nu \rightarrow Cl + CF_2Cl. \qquad (1\text{-}3)$$

Then, the Cl atoms will destroy ozone via a series of catalytic cycles, which is similar to the nitric oxide (NO) reaction chain discovered by Crutzen.[9] According to this photochemical model, one would expect that the place that receives the most sunlight (tropical area) should be the place that severest ozone depletion is observed. However, the observed ozone hole has been located in the lower stratosphere over the poles since 1985.[10] Then a mixed mechanism consisted of three major steps[11,12] was subsequently proposed. First, the Cl atoms produced by photolysis of Freons will react with other atmospheric molecules to generate other chlorine species (HCl and $ClONO_2$) in the tropical upper stratosphere. Second, air circulation will transport these chlorine species to the lower polar stratosphere, where chlorine (Cl_2) molecule is generated by the heterogeneous reactions occurring on ice surfaces in the polar stratospheric clouds (PSCs) during the winter:

$$HCl\ (s) + ClONO_2\ (g) \rightarrow Cl_2\ (g) + HNO_3(s). \qquad (1\text{-}4)$$

At last, reactive Cl atoms are released to destroy ozone from Cl_2 by the illumination of sunlight in the springtime.

1.1.2. The cosmic-ray-driven electron reaction (CRE) model

To understand CRE model for ozone depletion, essential knowledge of electron-induced reactions like dissociative electron attachment (DEA) and dissociative electron transfer (DET) will be illustrated first.

DEA is a well-known process in the interactions of electrons with molecules. It

happens when a molecule is resonantly attached by a low kinetic energy free electron (0-20eV) to form a transient anion state, and then anion state species dissociates into a neutral and an anionic fragment.[1] DEA can be described as following formula:

$$e^- + AB \rightarrow AB^{*-} \rightarrow A + B^- \qquad (1\text{-}5)$$

DEA process has been comprehensively reviewed by Sanche[13], Schultz[14] and Chutjian[15]. In contrast, dissociative electron transfer (DET) is a process when a localized electron (weakly bound to an atom or molecule) rapidly transfers to a foreign molecule forming a transient anion which then dissociates. In DET, no kinetic energy of the electron is involved. DET processes play important roles in many physical, chemical and biological systems as well as planetary atmospheres.[15,16,17,18,19,20] In this study, we will focus on the impact of electron-induced process in ozone depletion mechanism, particularly the electron induced adsorption of chlorine species on ice surface.

1.1.2.1. Introduction to CRE model

The major ozone-depleting molecules, chlorofluorocarbons (CFCs), have attracted the attention of scientists for a long time. In 1978-1979, Illenberger et al. found that dissociative electron attachment of gaseous CFCs to low kinetic energy free electrons is an extremely efficient process.

$$e^- \text{ (near 0 eV)} + CF_2Cl_2 \rightarrow CF_2Cl_2^{*-} \rightarrow CF_2Cl + Cl^- \qquad (1\text{-}6)$$

The measured DEA cross section of CF_2Cl_2 in the gas phase is four orders of magnitude higher than the photodissociation cross section.[21,22] Immediately, this DEA

of CFCs was considered as a potential mechanism for ozone depletion.[23,24]

In the stratosphere, the major source to produce electrons is atmospheric ionization by cosmic rays, which consist of protons and alpha-particles. Therefore, a large number of low energy secondary electrons are generated from ionized molecules entering the atmosphere. However, these free electrons are rapidly captured by atmospheric molecules to produce negative ions (mainly $O_2 \rightarrow O_2^-$). As a result, the detected density of free electrons is very low in the stratosphere. Because of the ineffective electron transfer from negative ions like O_2^- to CFCs, both DEA and DET of CFCs were regarded as not significant mechanisms for ozone depletion.[25,26] But according to the newest findings of DET process of CFCs when the water ice is present in Polar stratosphere clouds (PSC), the exclusion of DET mechanism for ozone depletion may be premature.

In 1999, Lu and Madey reported large enhancements in electron-induced dissociations of CFCs by the presence of polar media in the electron stimulated desorption (ESD) measurements.[27,28] This experiment can be described as follows. Submonolayer of CF_2Cl_2 was deposited on Ru (0001) substrate, which was then irradiated by a beam of electrons with energy at hundreds of electron volts. They found that the anions Cl^- and F^- were formed by DEAs to CF_2Cl_2 of low energy secondary electrons generated by the substrate after electron beam irradiation. Surprisingly, the yields of anions were enhanced significantly when CF_2Cl_2 was coadsorbed with polar media like H_2O and NH_3 as shown in Figure 1-1.

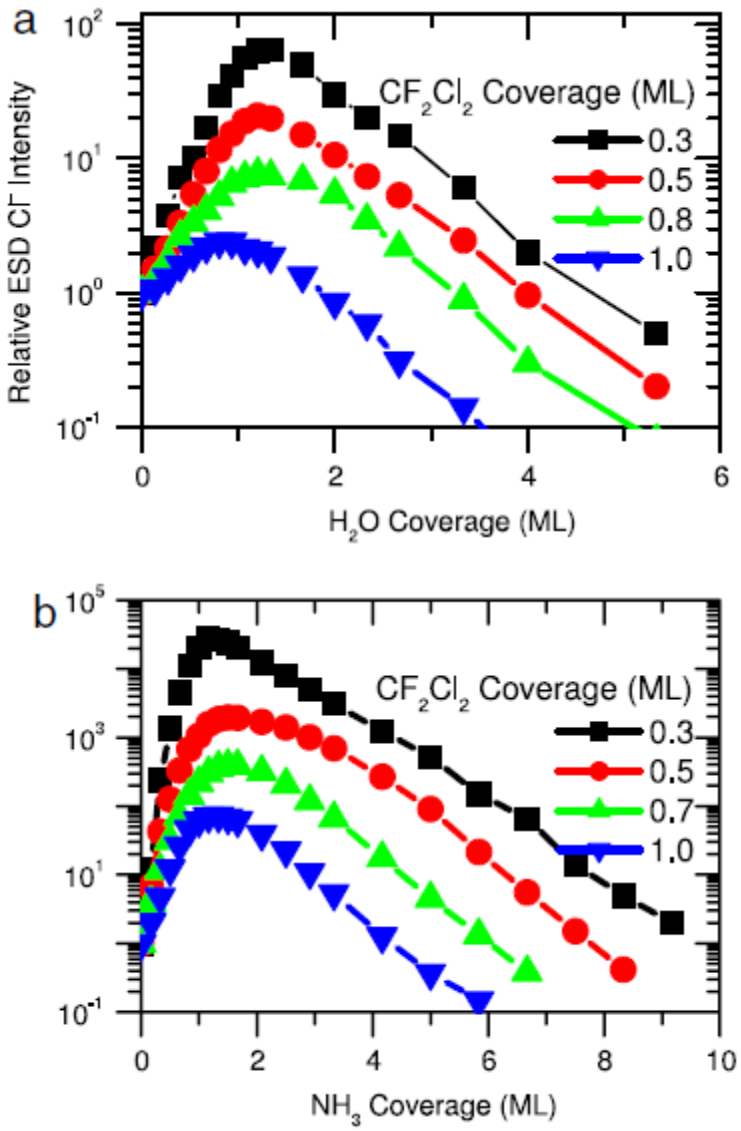

Figure 1-1 Relative Cl^- yields from electron stimulated desorption. The overlayers are (a) H_2O and (b) NH_3. Cl^- yields are normalized to the value with zero overlayer coverage.[27]

For the water overlayer, the Cl^- yields can be enhanced by close to 100 times at 1ML coverage. And the enhancement can be up to four orders of magnitude with 1 ML NH_3 overylayer.

Similar enhancements were observed when CF_2Cl_2 was adsorbed on top of polar medium (H_2O or NH_3) precovered Ru surface as Figure 1-2.

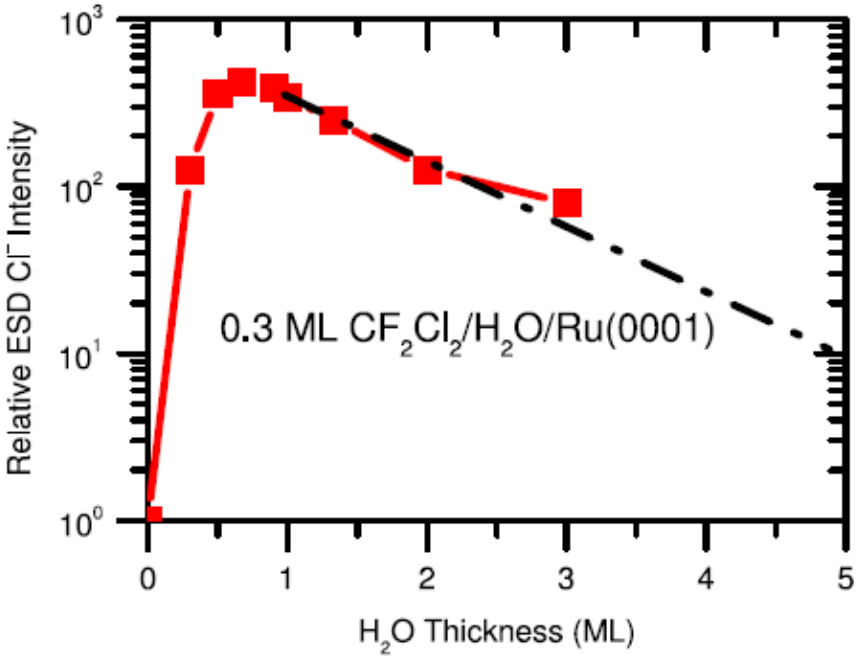

Figure 1-2 Relative Cl^- yields desorbing from 250eV primary electrons incident onto 0.3 ML CF_2Cl_2 adsorption on top of H_2O-precovered Ru substrate varying with H_2O spacer thickness. The dash-dot line is to extrapolate the Cl^- yield to the 5 ML H_2O spacer.[27]

The enhancement reaches its peak of two orders of magnitude when the spacer H_2O is one monolayer thick. With H_2O spacer gets thicker, Cl^- yield decreases due to the finite tunneling depth through H_2O film of low energy secondary electrons emitting from the substrate. In contrast, much smaller enhancements were observed when non-polar media (rare gas molecules) were used as spacer layer.[29,30]

Lu and Madey noticed that the excess electrons in polar media can stay in a precursor state (prehydrated electron) before the formation of solvated electron in equilibrium state for lifetime less than one picoseconds.[31] Based on this fact, Lu and Madey came up with a dissociative electron transfer (DET) mechanism to explain the large enhancements.[27,28] In the electron stimulated desorption (ESD) experiment done by Lu and Madey, secondary electrons from the metal substrate generated by primary electron are trapped in polar media first and then transferred to CFCs which dissociate consequently. The main reaction equations are present as follows.

$$e^- + mNH_3/nH_2O \rightarrow e_t^- (NH_3)_m / e_t^- (H_2O)_n \qquad (1\text{-}7)$$

$$e_t^- + CF_2Cl_2 \rightarrow CF_2Cl_2^{*-} \rightarrow Cl^- + CF_2Cl \qquad (1\text{-}8)$$

Considering that polar stratosphere clouds (PSC) consist of small ice particles exist in the polar atmosphere, where cosmic ray induced reactions can be dramatically different from general atmosphere without PSCs, the cosmic-ray-driven electron-induced reaction (CRE) model was proposed for ozone depletion by Lu[1,32,33]. Obviously, the in-situ CRE model is drastically different from the photochemical model.

In this model, secondary electrons generated by CR are trapped on the surfaces of ice particles. Then, these trapped electrons will be transferred to the chlorine species adsorbed on ice surfaces and make them dissociate to produce Cl^- ions as described in reaction equations 1-7 and 1-8. Some of these resultant Cl^- ions will be desorbed from ice particle surfaces and then participate in the following reactions[27] to release Cl atoms which can destroy ozone.

$$Cl^- + OH \rightarrow HOCl^- \qquad (1\text{-}9a)$$

$$HOCl^- + H^+ \rightarrow Cl + H_2O \qquad (1\text{-}9b)$$

$$Cl^- + NO_3 \rightarrow Cl + NO_3^- \qquad (1\text{-}9c)$$

$$Cl^- + HOCl + H^+ \rightarrow Cl_2 + H_2O \qquad (1\text{-}9d)$$

For those Cl^- ions which are still adsorbed at the surface of PSCs due to the image potential,[27] they can further react with other species to release photoactive species like Cl_2 or $ClNO_2$, which will release Cl atoms to destroy ozone when spring comes. These steps can be described by following equations:[27]

$$Cl^- + ClONO_2 \rightarrow Cl_2 + NO_3^- \qquad (1\text{-}10a)$$

$$Cl^- + N_2O_5 \rightarrow ClNO_2 + NO_3^- \qquad (1\text{-}10b)$$

$$Cl^- + HNO_3 \rightarrow HCl + NO_3^- \qquad (1\text{-}10c)$$

The second reaction channel (equation 1-10) is believed to dominate over the first reaction channel (equation 1-9) because of the low desorption probability of Cl^- ions.[27]

1.1.2.2. Other justifications for CRE model

The DET mechanism for CRE model has been justified by varieties of experimental methods, such as the electron stimulated desorption measurements[29,30], electron trapping measurements[32,34,35,36] and femtosecond time-resolved laser spectroscopic measurements.[37,38] Specifically, a large enhancement in photodissociation of $CFCl_3$ coadsorpted with thin ice film was observed by Ryu et al. in 2006. As shown in Figure 1-3, they found that lifetime of solvated electrons is a function of $CFCl_3$ coverage.

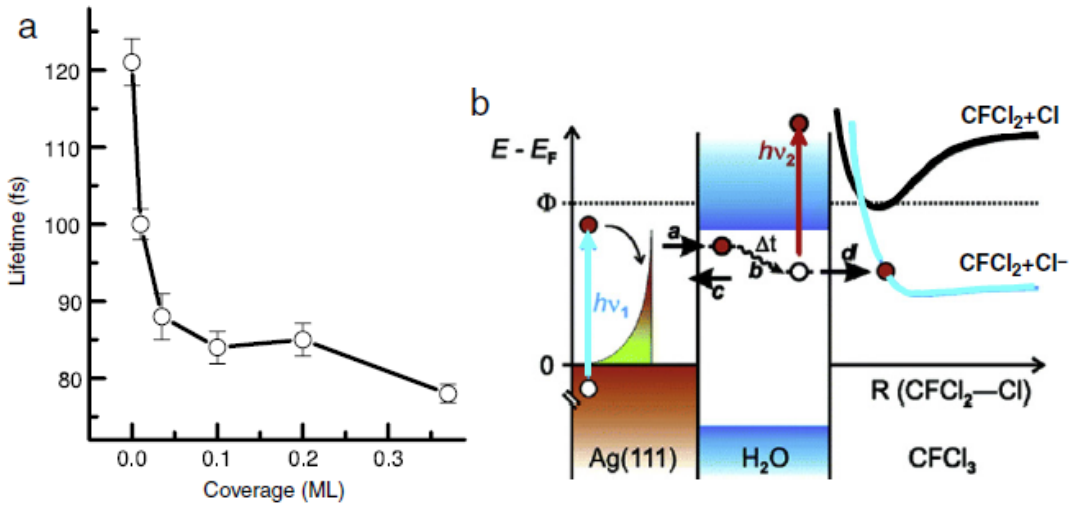

Figure 1-3 (a) Lifetime of the pre-solvated electrons as a function of the coverage of $CFCl_3$ adsorbed on 5 ML H_2O/Ag (111). (b) Schematic diagram for the life cycle of the photoinjected electrons in $CFCl_3$ / H_2O /Ag(111): photoinjection of electron into the loosely bound e_{pre} state residing below the vacuum level(a); solvation in the ice layer (b); back

transfer of the photoinjected electron to the metal (c); electron transfer to coadsorbed $CFCl_3$ (d).[38]

Significant decrease in lifetime reveals pre-solvated electrons are scavenged by $CFCl_3$ very quickly. It is believed that the pre-solvated electrons in ice film, which were generated from substrate by primary photons, transferred to coadsorpted $CFCl_3$, leading to the dissociation of $CFCl_3$.[38]

In addition, the lifetimes of presolvated electrons on ice were under debate before 2008. But Wang et al. found that lifetimes of electrons at two presolvated states in liquid water were about 200fs and 500fs respectively, after the identification and removal of a coherent spike generated by time-resolved laser pump-probe spectroscopic measurements.[39] Under the temperature condition of PSCs (about 180K), a theoretical model was proposed by Baletto et al for the surface trapped excess electrons on ice.[40] It is proposed that surface trapped excess electrons will cause rearrangement of surface H_2O molecules. More dangling OH bonds will point toward the vacuum to create an electrostatic field which prevents the decay of excess electrons being solvated by bulk H_2O molecules. Recently, Bovensiepen et al. showed the reactivity of water-electron complexes on crystalline ice surfaces. Interestingly, they found the lifetime of excess surface electrons can be up to minutes and that these excess electrons will be efficiently transferred to $CFCl_3$, leading to molecule dissociation.[41]

As we know, ice particles in PSCs are mainly crystalline instead of amorphous. Therefore, the interactions between chlorine species and water ice with different morphologies have been investigated.[42,43,44] In 2001, Lu et al. showed structural and temperature effects on Cl^- yields in electron-induced dissociation of CF_2Cl_2 adsorbed on ice.[45] Specifically, it is reported that a non-Arrhenius temperature dependence of Cl^- yield is observed on crystalline ice. The Cl^- yield at 190K (PSC temperature) is expected to be about three orders higher than the value at 25K by fitting experimental data into Vogel-Fulcher-Trammann (VFT) equation.[45,46,47] Most recently, Bovensiepen

et al.[41] and Martin Wolf et al.[48] also confirmed high reactivity of surface trapped electrons on crystalline ice, leading to a large dissociation of $CFCl_3$. Thus, it can be concluded that trapped electrons transferring from crystalline ice to CFC molecules can occur efficiently in PSC conditions.

These results mentioned above further confirm the fact that dissociation of Freon species in PSC can be caused by DET reactions driven by cosmic rays.

1.1.2.3. Spatial and time correlations between cosmic rays and ozone depletion

If CRE mechanism plays the leading role in ozone depletion, then the correlation between cosmic ray intensity and ozone depletion should be observed. Indeed, after they analyzed the data acquired from satellites, Lu and Sanche[32] found a strong spatial correlation with variations of latitude and altitude as Figure 1-4.

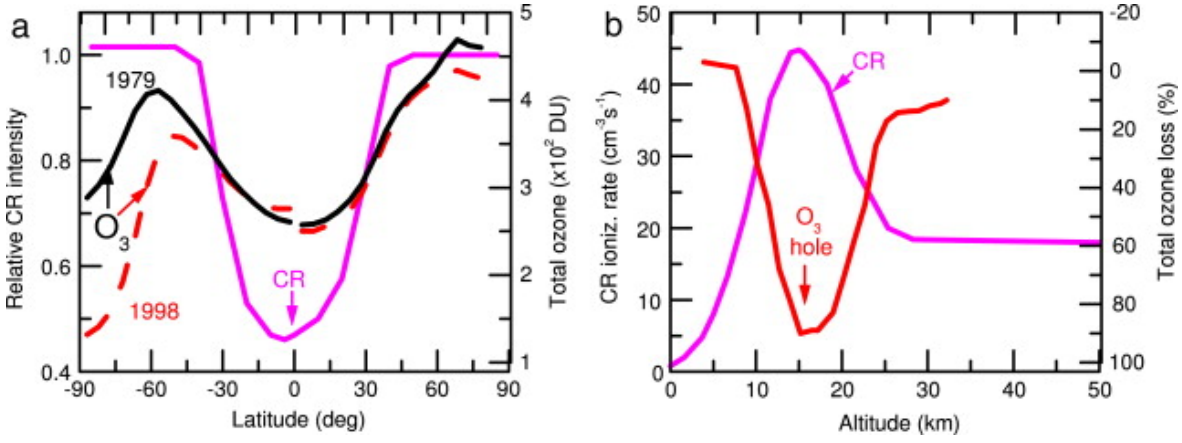

Figure 1-4 Space correlations of cosmic ray intensity and monthly mean total ozone.[32]

Figure 1-4(a) shows a latitude correlation between CR intensity and ozone depletion. Large depletions are observed at polar areas that receive the most intensive CRs. But

no change of ozone concentration is observed at tropic area where CR intensity stays at a very low level. As depicted in Figure 1-4(b), an obvious altitude correlation can be found. The position (altitude 15-18km) where CR ionization rate is highest is the place where the ozone hole is observed.

Recently, Dr. Lu[33] has shown a strong correlation not only in the southern hemisphere (0-60°S) but also in the Antarctic ozone hole (60-90°S) between satellite data for mean total ozone and over two 11-year cosmic ray cycles (1979-2007) as Figure 1-5.

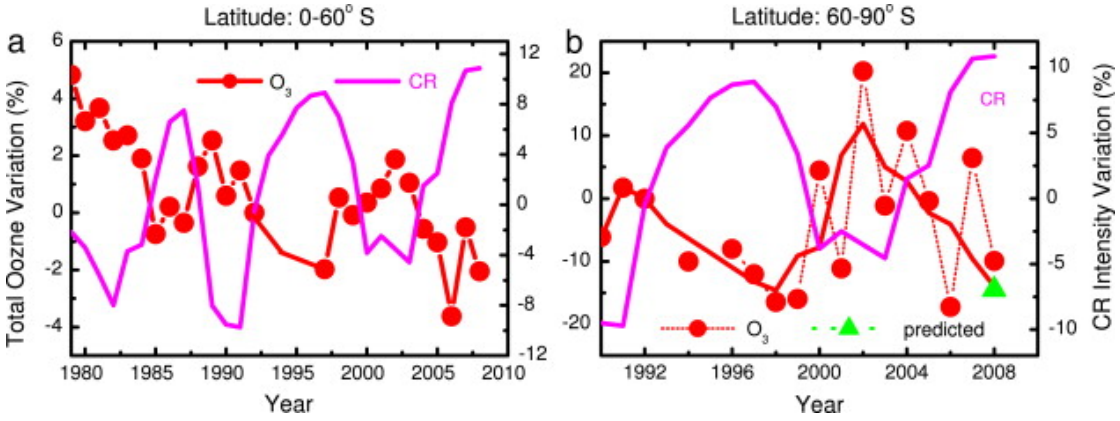

Figure 1-5 Time correlations of Percentage variations of observed CR intensity and annual mean total ozone.[33]

According to CRE mechanism, the ozone depleting reactions are dependent on halogen concentrations (EESC), the intensity of cosmic rays (I) and the amount of PSCs for trapping the electrons. Taking the stratospheric cooling[1] caused by polar ozone loss in the preceding year into account, Lu came up with an equation for the steady-state total ozone ($[O_3]_i$) in the Antarctic in spring as[1]

$$[O_3]_i = [O_3]_0 [1 - k \times I_i \times I_{i-1} \times EESC_i], \qquad (1\text{-}11)$$

where $[O_3]_0$ is the total ozone in polar stratosphere when EESC = 0, I_i the CR intensity in the ith year and k a constant.

In 2010, confirmation of the 11-year cyclic ozone loss over spring Antarctica was reported as shown in Figure 1-6.

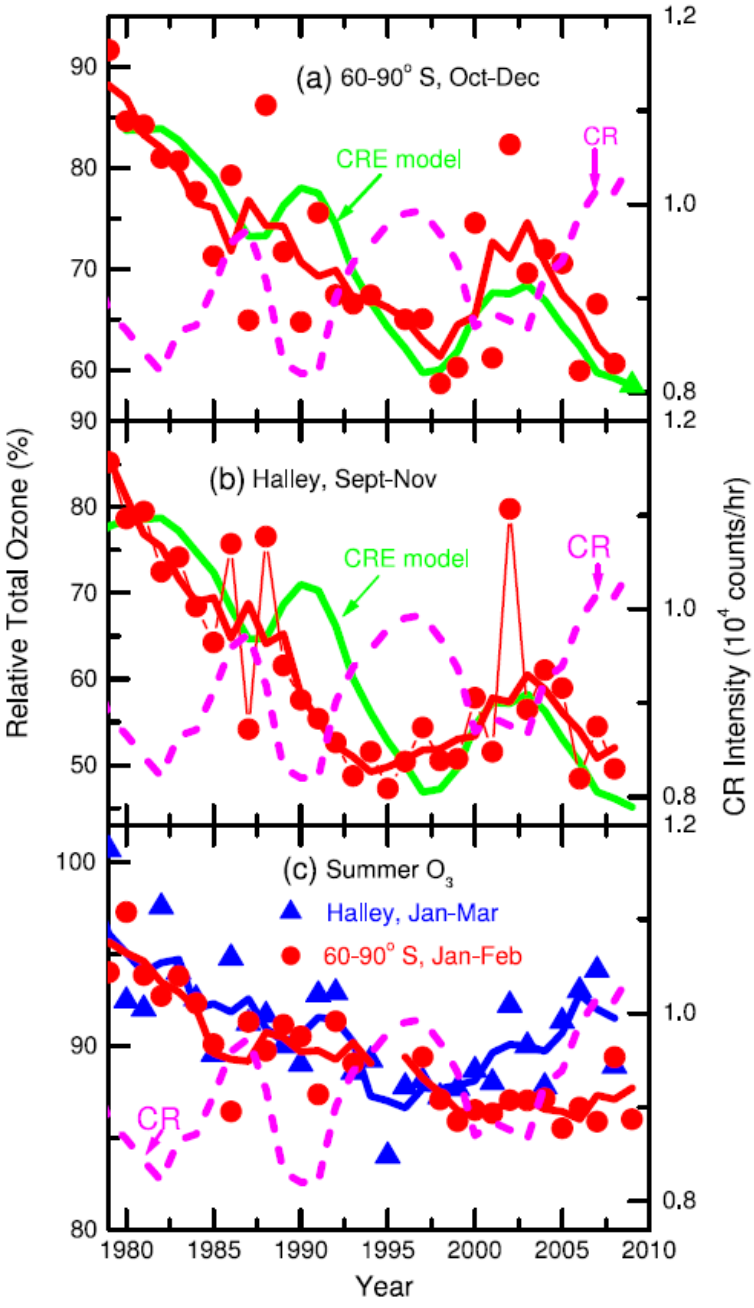

Figure 1-6 (a) Percentage of spring zonal mean total ozone over Antarctica with latitudes of 60-90°S and cosmic ray (CR) intensity variation during the period of 1979-2008, as well as total ozone variation given by the CRE model Eq. (1-9) with $k = 2.1 \times 10^{-9}$. The CR data were obtained from the measurements at McMurdo (77.9° S, 166.6° E). The upper triangle is the predicted by Eq. (1-9). (b) Similar to (a), but the ozone data were obtained from the Antarctic Halley (75°35′ S, 26°36′ W) and averaged from September to November, normalized to $[O_3]_0$ = 300 DU; the calculated ozone data were obtained by Eq. (1-9) with $k = 2.8 \times 10^{-9}$. (c) The summer zonal mean total ozone (solid circles) at 60-90°S averaged from January and February and the summer ozone

data (solid triangles) at Halley averaged from January to March, normalized to $[O_3]_0$ = 320 DU. In (a)-(c), the fine solid lines through the data points are three-point average smoothed curves to aid the eyes.[1]

The correlations can be clearly seen from Figure 1-6(a) and 1-6(b) for spring time but no correlation exists in the summer (no PSCs) as showed in Figure 1-6(c). Above all, it can be seen that newly proposed CRE mechanism[1] for ozone depletion can fit these observed data very well.

1.1.3. Electron induced adsorption

In the CRE model for ozone depletion, the in situ electron induced reaction of chlorine species adsorbed at ice particles in polar stratospheric clouds is the key step for the formation of photoactive halogen species, which will destroy ozone in the spring.[1] The large enhancements in electron-induced dissociation of chlorine species on ice have been reported by Lu and others.[18,38,41] However, the adsorption process of chlorine species on ice surface, as a precondition for all the following reactions, has not been studied extensively. Therefore, the major object of this project is to investigate the adsorption of chlorine species on ice surfaces.

In the polar stratosphere, an enormous number of low energy secondary electrons can be generated by intense cosmic rays. These secondary electrons are captured quickly by the atmospheric molecules and make the PSC ice charged. The charged PSC ice surface would have different physical and chemical properties from normal ice surface. Thus, it is necessary to study the chlorine species adsorption process on charged ice surface.

1.2. Electron involved surface phenomena

In this section, electron involved phenomena, e.g. adsorption and desorption as well as electron-induced reactions will be discussed.

1.2.1. Electron-induced adsorption and desorption

Compared to normal adsorption, the process of electron-assisted adsorption could be significantly different and complicated. For example, oxygen gas molecule can only be physisorbed on a gold surface in normal condition. But it will undergo chemisorbtion if the gold surface is irradiated by an electron beam. In order to understand electron-assisted adsorption, a lot of studies have been carried out.[49,50,51] In practice, people can take advantage of this phenomenon to control the deposition process. Particularly, electron-beam-induced-deposition (EBID) technique has been widely used in nanofabrication even though this process was not fully understood when the technique was first invented. The basic principle of EBID is described as follows. The substrate with adsorbed precursor species is irradiated by a focused electron beam. After a series of electron induced reactions, the precursor species will dissociate into deposited molecules and volatile fragments. The latter will be pumped out quickly. Interestingly, many EBID studies show the lateral size of the deposited material obviously exceeds the diameter of the electron beam.[52,53,54] Surface migration was postulated by Vignes et al. as the potential reason for the large area of contamination. But later, H.T. Liu and Z. Wu showed that it is secondary electrons, instead of surface migration, that are responsible for the extended area of adsorption.[55] In 2002, a complete theoretic model for the role of secondary electrons in EBID was first introduced by N. Silvis-Cividjian et al. The predictions of this model are

consistent with experimental observations.[56]

Conversely, electrons can also play an important role in desorption processes. Electron-induced desorption (ESD) is a widely used technique in surface science. In ESD, a surface adsorbed species can be electronically excited to an ionic state by accepting energy from impinging electrons. The excited species may attain enough kinetic energy to leave the surface when they relax from an excited state to the ground state. Unlike low energy electron diffraction and Auger electron spectroscopy, which are plagued by the electron beam damage to the surfaces being studied, ESD is a very powerful tool to characterize adsorbed species on surfaces by using the electron beam itself. This technique has been comprehensively reviewed by Yates and Madey in 1971.[57]

Extensive studies have been done to investigate the electron involved reactions as well as adsorption and desorption processes on metal or silicon surfaces in response to the rapid growth of the semiconductor industry in last few decades. Even though great attention has been paid to dynamics of solvation electrons in aqueous environments, the electron induced adsorption on water or ice surface, which is also an important factor in environmental, interstellar, and biological chemistry, has not been fully studied yet. Thus, the major aim of this project is to investigate adsorption phenomena on charged ice surfaces. A potassium doped ice surface was used in this project to achieve a charged surface due to the self-ionization of potassium atoms.[58]

1.2.2. Electron-induced reactions of carbon tetrachloride (CCl_4)

The impact of chlorocarbons on environment and human health has been attracted attention since chlorine species are widely used in industry. In fact, a lot of

chlorocarbons do not degrade easily under ambient conditions.[59,60] As a result, many chlorocarbon degradation techniques have been developed over the past several decades.[61,62,63] A number of studies have been carried out to investigate the decomposition of chlorocarbons and Freon under electron irradiation. In 1970s, DEA to halomethane in gas phase was reported by Illenberger et al. The halomethane molecules were impacted by low energy electrons (0-10eV) and an extremely high yield of Cl^- was found when the incident electron energy was near 0eV.[21,22,64] Taking CCl_4 as an example, it can capture a low energy electron and form negative ion resonance (NIR), then dissociates into a radical and an anion as follows:

$$e^- + CCl_4 \rightarrow CCl_4^{*-} \rightarrow .CCl_3 + Cl^- \qquad (1\text{-}12)$$

The lifetime of the CCl_4^{*-} transition state was determined to be several picoseconds by Wang et al.[65] in liquid and Popple et al.[66] in the gas phase independently.

1.3. Enhanced gas adsorption on charged surface

H. M. van Driel's group reported the observation of common gases like He, Ar, H_2, O_2, N_2, CO adsorbed on silicon oxidized surfaces at room temperature.[7,67,68] The contact potential difference (Kelvin probe) technique is used for work function measurements. Results are shown in Figure 1-7.

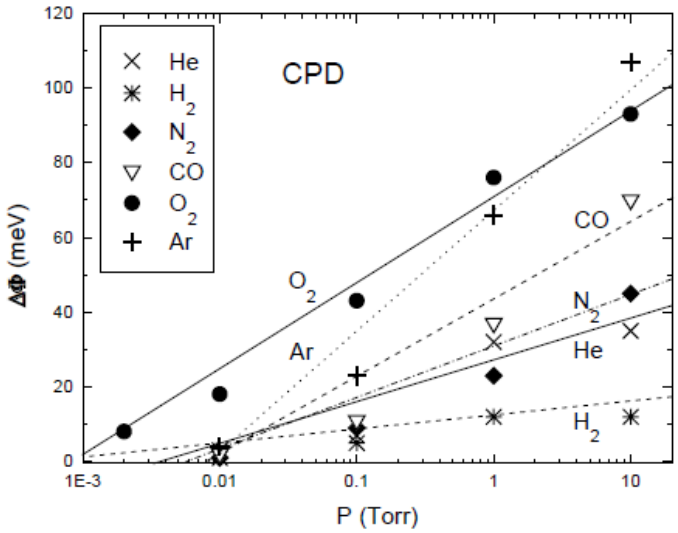

Figure 1-7 Work function changes with different exposure pressures.[7]

The observed results show similar changes of work function for all gases, indicating the mechanism for gas adsorption must be the same. Thus, they proposed a universal electrostatic coupling mechanism in which the gas molecules get polarized first by the surface negative charges that create an electrostatic field of the order of several volts per nanometer.[7] Then polarized gas molecules are adsorbed on the surface by electrostatic binding and adsorption is assisted by field-induced chemisorption.

In addition, they showed the adsorption can get enhanced if the surface is more negatively charged by internal photoemission current (PEC) when the sample was illuminated by a laser beam. Before gases were introduced into the chamber, PEC of a clean sample was measured as a reference for normalization. Then the laser beam was turned off and gases were admitted into the chamber at pressure 0.1 torr. After about 1

minute gas exposure, the laser beam was turned on again and PECs were recorded. Results are shown in Figure 1-8.

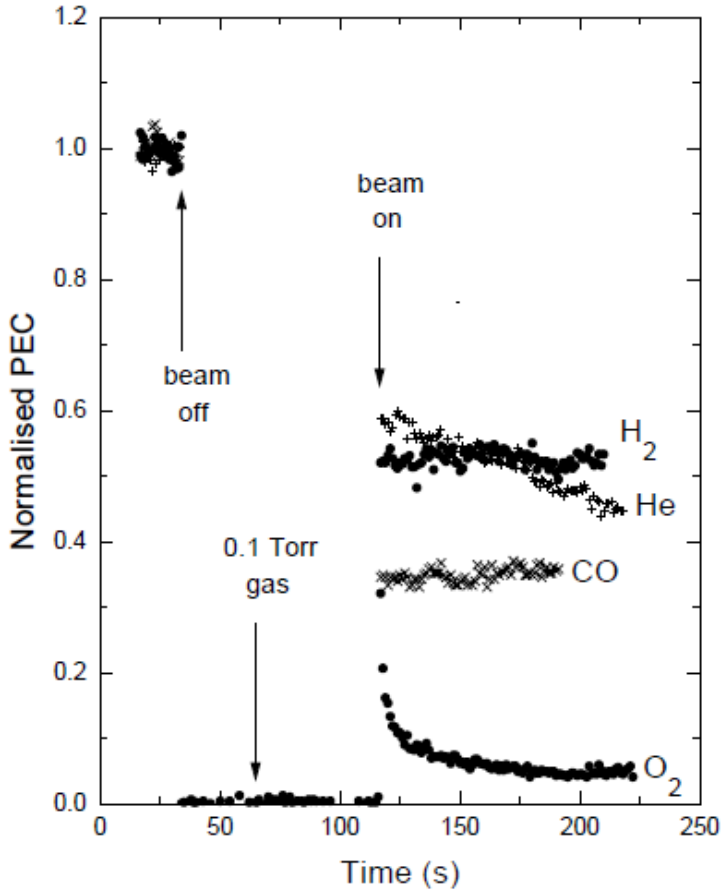

Figure 1-8 Photoemission current before and during exposure to 0.1 torr of different gases.[7]

These results confirmed that negative surface charges have significant influence on gas adsorption. Also after introducing gases to the analysis chamber, a decrease of photoemission current (PEC) can be observed for all gases.[7,67,68] The decrease of PEC indicates the surface becomes more negatively charged. Conclusively, adsorption of gases and the surface charging are mutually enhanced by each other.

Considering this project, it is possible that CCl_4 molecules could be adsorbed on the ice surface and that adsorption gets enhanced by negative charges on ice surface due to the universal mechanism of gas adsorption just mentioned above. However, the microstructure of ice surface like roughness could also affect this adsorption process.

This effect is discussed in section 1.5.

1.4. Charged ice surface

In the study of CCl_4 absorption on ice, a charged ice surface is needed to compare with the uncharged surface. The charged surface can be simply achieved by doping low coverage alkali metal atoms on ice surface. The principle of this method will be explained here.

Photoemission of alkali metal doped ice at low coverage has been investigated by Steve Meech's group[69,70]. All three alkali metals (Li, Na, K) can cause a dramatic decrease in the photoemission threshold of ice-vacuum interface.[58] Interestingly, this threshold is even lower than that of pure alkali metals in gas phase. This observation has been ascribed to the formation of a metastable and incompletely delocalized surface trapped electron stabilized at the ice-vacuum interface with a lifetime from several hundreds to a few thousands seconds depending on the temperature.[58,70] During the lifetime of these metastable surface electrons, they are loosely associated with their parent alkali metal atoms and not completely solvated by H_2O.

In addition, quantum chemistry calculations have been carried out for interactions of alkali atoms and ice molecules.[58,70] The calculated structures of interaction between potassium atom and H_2O molecules are shown in Figure 1-9.[70]

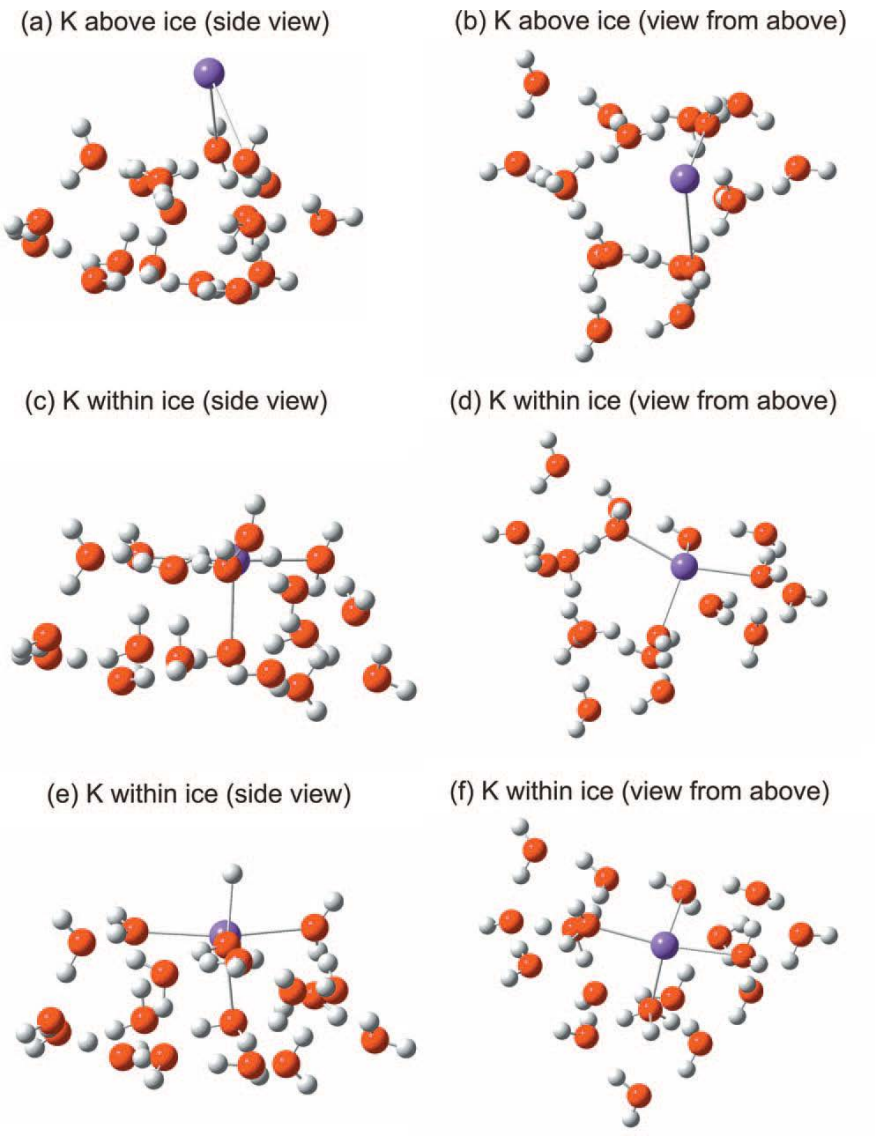

Figure 1-9 Model of potassium atom interaction with 18 H_2O. The red large spheres are O atoms, the white small spheres are H atoms, and the big purple sphere is K atom.[58]

The calculations are quite consistent with experiment results. Figure 1-8(a) and 1-8(b) show the K atom bound above the H_2O surface as the potassium atom approaches the H_2O molecules. At this stage, the K atom is just loosely bounded. Figure 1-8(c) and 1-8(d) show that the K atom is more strongly bound within the H_2O surface. Figure 1-8(e) and 1-8(f) show the K atom has been almost fully ionized. The K 4s electron is now delocalized to an H_2O molecule so that an H atom stretches above the surface. Such stretched H atoms may recombine with each other and then leave the surface as H_2. Then K will be fully ionized in the ice.

Recently, a study of low energy charged particles interacting with amorphous solid water (ASW) has been carried out. It is reported that negative charges can be trapped by intrinsic surface defects and solvated electrons preferentially reside near the ASW-vacuum interface with a lifetime of hours.[35,71] From these experiment results, self-ionization of the surface adsorbate can serve as an electron donor to make the surface charged.

1.5. Surface of ice films

The ice surface is attracted intense research interest since it is involved in many physical and chemical interactions of biological, environmental, interstellar systems. Properties and structures of ice surface are briefly addressed here.

According to morphology, ice can be generally categorized as two types, amorphous and crystalline ice. The formation of different types of ice is dependent on the deposition conditions. Usually, crystalline ice is formed when the deposition temperature is higher than about 130K and the formation of amorphous ice needs temperature lower than about 130K.[72] Extreme low temperature and high deposition rates will lead the formation of microporous amorphous ice. On the other hand, pore-free solid amorphous ice is formed with low deposition rates from collimated dosing sources at normal incidence independent of temperature.[73] These kinds of ice exhibit very different surface properties.

In our project, the surface of ice film is the place where adsorption happens so that it is of great importance to know the ice film surface structure. A study of interactions of carbon tetrachloride (CCl_4) and thin D_2O amorphous ice films[74] has been carried out by W. Ronald Gentry et al. Temperature-programmed desorption (TPD) method was applied in their experiment. It is shown that two-dimensional islands of CCl_4 are formed on the solid amorphous ice surface for low CCl_4 exposure. But three-dimensional CCl_4 clusters are observed to be trapped in the pores of microporous ice rough surface. Desorption of such trapped CCl_4 clusters requires high desorption temperatures (180 - 190 K). Kay et al. also investigated desorption of CCl_4 on amorphous solid water (ASW).[75] They found that desorption of CCl_4 film would be completed before the onset of significant water desorption. And in the case of CCl_4 film covered by ASW overlayer, Kay et al. discovered the abrupt CCl_4 desorption at about 160 K due to the crystallization of ASW.[75] Therefore, the CCl_4 desorption peaks

of TPD spectra indicate resident state of adsorbed CCl_4 on surface and their desorption pathways. Conversely, CCl_4 can be used as a probe to investigate ice structures.

Chapter 2

Experimental method

All experiments were performed in a vacuum chamber. The major techniques applied in this project are temperature programmed desorption and Kelvin Probe work function measurements. These two techniques are very common in surface science research and will be explained in detail in this chapter. A brief review of the fundamental principles of surface science will be presented first.

2.1. Fundamental principles

In this section, fundamental principles of surface science such as chemisorption and physisorption, adsorption and desorption kinetics, and the Langmuir adsorption model will be briefly reviewed.

2.1.1. Chemisorption and physisorption

Adsorption is a process when the attractive interaction between a particle and a surface is strong enough to overcome the disordering thermal motion of the particle and makes the particle residual on the surface. The adsorption process is often classified as physisorption and chemisorption.

Physisorption is a result of attractive interaction of van-der-Waals forces between adsorbate and adsorbent. This process doesn't involve significant change in the species electronic orbital. Physisorption is not specific. Almost all gases can be physisorbed to almost all surfaces under certain conditions. Physisorption usually occurs at low temperature and also can occur as a preliminary state to chemisorption.

Chemisorption takes place when chemical bonds are formed at a surface. Molecular orbitals of the adsorbate and adsorbent will overlap each other. Chemisorption is often an activated process which requires that an activation barrier is overcome. A dissociation of the adsorbate is often observed at the same time with chemisorption, for example, oxygen molecules will dissociatively chemisorb on most metal surfaces at room temperature.

2.1.2. Adsorption kinetics

From the kinetic theory of gases, the flux I of gas molecules colliding on the surface from the gas phase is given by[76]

$$I = \frac{p}{\sqrt{2\pi m k_B T}} \qquad (2\text{-}1)$$

Where m is the mass of the gas molecule, k_B is Boltzmann's constant, T is the temperature and p is the partial pressure of the adsorbing gas.

However, the surface cannot adsorb all impinging molecules. Therefore, the adsorption rate will be different from impingement rate. And the ratio between them is defined as the sticking coefficient, s. Thus, the adsorption rate r_a is

$$r_a = sI \qquad (2\text{-}2)$$

In activated adsorption, the sticking coefficient is expressed as

$$s = \sigma f(\boldsymbol{\Theta}) \exp(-E_{act}/k_B T), \qquad (2\text{-}3)$$

where σ is called the condensation coefficient, **Θ** is the coverage of adsorbate, $f(\boldsymbol{\Theta})$ is a coverage dependent function which gives the probability of finding an adsorption site.

2.1.3. Langmuir Adsorption Model

The Langmuir adsorption model is the simplest and most commonly used model for adsorption. It is based on the following assumptions:

- All adsorption sites are equivalent.
- Adsorption is limited by monolayer coverage.
- No interactions between the adsorbed particles.
- One adsorption site can only adsorb one molecule and the adsorbed particles are immobile.

In general, the Langmuir adsorption model can be classified as non-dissociative Langmuir adsorption and dissociative Langmuir adsorption. Note that the dissociation of molecules can be suppressed by lowering the surface temperature, i.e. O_2 adsorption on a metal surface.

For non-dissociative Langmuir adsorption[76],

$$f(\Theta) = 1 - \Theta \qquad (2\text{-}4)$$

And the Langmuir adsorption kinetics is written as

$$\frac{d\Theta}{dt} = s_0 I(1 - \Theta), \qquad (2\text{-}5)$$

where s_0 is the sticking coefficient at zero coverage.

For dissociative Langmuir adsorption[76],

$$f(\Theta) = (1 - \Theta)^n, \qquad (2\text{-}6)$$

where n stands for the order of the kinetics.

2.1.4. Desorption kinetics

Thermal desorption is the process in which adsorbed species gain enough energy to escape from the surface. Desorption is usually described by the term desorption rate, r_{des}, which gives the number of particles desorbing from unit surface area per unit time.

Under the assumption that there is no interaction between adsorbed molecules, the desorption rate can be written as the Polanyi-Wigner equation:

$$r_{des} = -\frac{d\Theta}{dt} = k_n \Theta^n \exp(-E_{des}/k_B T) \qquad (2\text{-}7)$$

Where E_{des} is the activation energy of desorption, n the order of the desorption, and k_n the desorption rate constant.

In zero-order kinetics (n=0), the desorption rate doesn't depend on coverage. It happens at desorption of a homogeneous multilayer film. In first-order kinetics (n=1), the desorption rate is proportional to coverage. It happens when atoms desorb from their sites directly. In higher order kinetics, the desorption rate is proportion to Θ^n. This indicates associative molecular desorption.

2.2. Temperature-Programmed Desorption method

Temperature-programmed desorption (TPD) techniques are widely used in surface analysis. The purpose of this method is to determine kinetic and thermodynamic parameters of desorption processes or decomposition reactions. A sample is contained in an ultra-high vacuum (UHV) and it is heated with a temperature program. Usually, the temperature is a linear function of time. When the temperature rises, a particular adsorbate species will have enough energy to leave from the substrate surface. Meanwhile, the residual gas in the vacuum is detected simultaneously by a mass analyzer and the signal is usually recorded. Then a plot of desorption rate versus temperature can be made. The peak temperature will provide information on the desorption kinetics.[76]

In most TPD experiments, temperature is a linear function of time,

$$T(t) = T_0 + \beta t, \qquad (2\text{-}8)$$

where t is the time and β is the heating rate.

In general, the desorption peak temperature T_{max} is related to desorption energy E_{des}. Redhead derived a relation between E_{des} and T_{max}:

$$E_{des} = k_B T_{max}(\ln\frac{v_1 T_{max}}{\beta} - \ln\frac{E_{des}}{RT_{max}}) \qquad (2\text{-}9)$$

The second part in brackets is estimated[77] as 3.64 and resulting in:

$$E_{des} = k_B T_{max}(\ln\frac{v_1 T_{max}}{\beta} - 3.64), \qquad (2\text{-}10)$$

where v_1 usually takes value 10^{13} s^{-1}.[77]

2.3. Kelvin probe method for work function change measurements

In this section, an introduction to the Kelvin probe method will be presented first. Then a temperature-programmed work function measurement technique will be illustrated.

2.3.1. Introduction to Kelvin probe

The work function of a certain substance is defined as the minimum energy required to extract one electron from the surface of this substance, that is to say, the energy difference between the vacuum level and the Fermi level as shown in Figure 2-1.

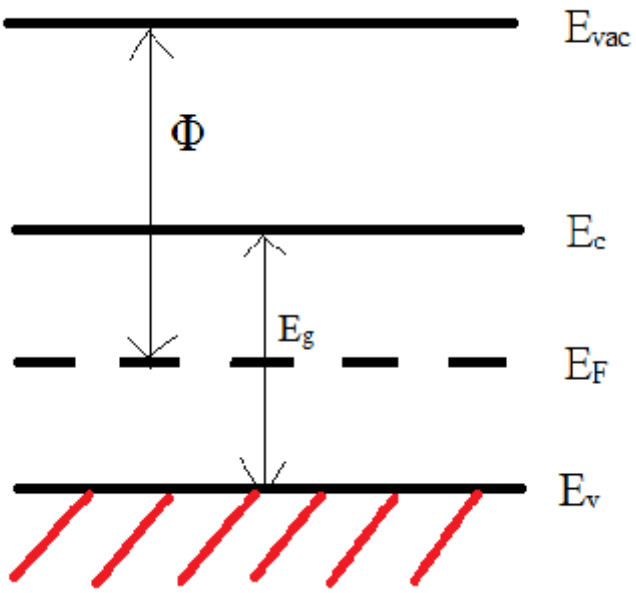

Figure 2-1 General band and diagram with the vacuum level E_{vac}, the conduction band E_c, valence band E_v, band gap E_g.

As we know, each kind of material has its unique work function. If some particles of other species are adsorbed on its surface, the electronic structure of the surface changes and so does the work function. Taking advantage of this phenomenon, the

adsorption process of a surface can be observed by analyzing the surface work function change.

The Kelvin probe method, which is one of the most popular techniques for measuring work functions, is applied in this experiment. A schematic diagram of Kelvin Probe is shown in Figure 2-2

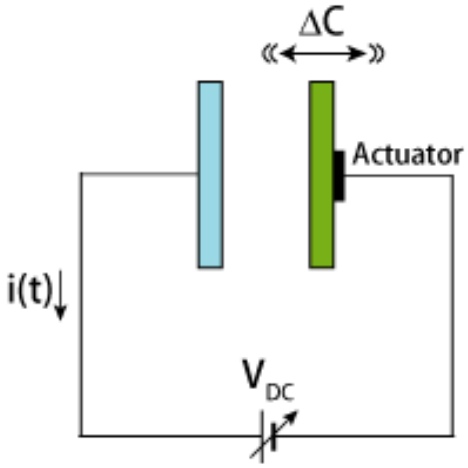

Figure 2-2 Schematic diagram of Kelvin probe. The blue plate is the sample and the green plate is the probe mesh.[78]

As shown in Figure 2-2, the capacitor is formed by the probe and sample. If the probe is vibrating at certain frequency, the capacitance will be changed periodically, leading to an AC current in the circuit.[76]

$$i(t) = \frac{\Delta C}{\Delta t} U = \frac{\Delta C}{\Delta t} (\Delta \emptyset / e + \mathrm{V_{DC}}), \qquad (2\text{-}11)$$

Where C is the capacitance, $\Delta\emptyset$ is the potential difference between sample and probe and V_{DC} is the bias voltage.

By adjusting the voltage V_{DC}, the current can be set to zero no matter how capacitance is changed. The condition is:

$$\mathrm{V_{DC}} = -\Delta \emptyset / e. \qquad (2\text{-}12)$$

Once V_{DC} is known, the work function of the sample relative to the reference probe will be obtained.

The work function change is obtained by comparing the DC biases before and after deposition of certain species on the sample surface. The DC bias can be adjusted in both manual and auto modes of the controller.

2.3.2. Work function change measurements with varying temperature

In some of our experiments, the measurements of work function change are constantly recorded during the time when the temperature is varying, either heating up or cooling down. This technique allows us to observe the work function change simultaneously at different temperatures. Information of adsorption or desorption processes can be investigated from the plot of work function change verse temperature. Usually, the temperature increase or decrease is not linear with time. But the data can only be recorded as a function of time by the computer. Then the temperature will be recorded every 10 seconds manually such cases. Thus, work function change of the sample can be measured as a function of not only time but also temperature.

2.4. Ultrahigh Vacuum (UHV)

2.4.1. UHV chamber

The UHV chamber is the central part of the vacuum system and is made from high grade steel which has the properties of low gas permeability and resistance to corrosion. Conflat flanges are used for all mountable parts. Every conflat flange has a knife edge that affords a seal by cutting into a copper ring (gasket). The following equipment is installed to the chamber and was used for the experiment.

- A mechanical dry pump.

  The mechanical dry pump is a compact, reliable vacuum pump which can bring the pressure down to 10^{-3} torr.

- A turbomolecular (turo) pump.

  This pump operates in the range from 10^{-3} to 10^{-8} torr.

- An ion pump.

  This ion pump starts to operate at about 10^{-8} torr and has the ability to reach the 10^{-10} torr level.

- A Titanium sublimation pump.

  Titanium sublimation is used intermittently in addition to the ion pump. Titanium is sublimated from the filament and reacts with residual active gases in the chamber to form non-volatile compounds which will be exhausted out very quickly. Note that the titanium sublimation pump should not be used when the

sample substrate is at low temperature in case the cold substrate surface will be contaminated by titanium atoms which are very difficult to remove from copper substrate.

- Three pressure gauges.

  No single gauge has the ability to operate in the entire range from atmospheric pressure down to utra-high vacuum. Therefore, three different types of gauges are used to measure the pressure. They are a mechanical gauge, a thermocouple and an ionization gauge which are all connected to a multi-gauge controller to monitor the pressure in the chamber.

- Three viewports.

  The three viewports are transparent for visible light (made of glass). They allow the researchers to view the vacuum process from different angles.

- Two leak valves.

  Leak valves can control the amount of gases dosing into the chamber. In this particular experiment, one valve is used for dosing H_2O (directional), and another is used for dosing CCl_4 (background). Several freeze-pump-thaw cycles had been applied to H_2O/CCl_4 containing tubes for degassing before the leak valves were opened.

- A translator.

  A sample substrate is mounted onto this translator, which can manipulate the sample in three dimensions with high precision. A liquid nitrogen cooling reservoir is mounted at the back of the sample holder and in connected by a liquid feedthrough. Sample temperature can be lowered down to 90K by introducing liquid nitrogen into the liquid feedthrough. Also, the sample can be heated by applying a current to a filament at the back of the sample. The substrate can be

cleaned by heating up to 900K for several cycles. To obtain such high temperature, it is necessary to apply high positive voltage to the sample so that the electrons from the filament will bombard the substrate with much higher energy. Note that varying supply current to the filament can regulate the temperature rate of increase β, which is an important parameter for the TPD experiment.

- A quadrupole mass spectrometer (QMS).

  The QMS is able to identify the species and relative intensities of the residual gases in the vacuum chamber. The scan width and scan center are adjustable from 1 to 300 AMU. The data can be recorded and displayed by a computer.

- A Kelvin probe with its controller.

  Work function changes of the sample can be measured by the Kelvin probe operated by a controller. The electrode of the Kelvin probe is a metallic mesh connected to HI on the controller with a shielded cable in vacuum. A reference electrode is also mounted on this probe and connected to IN on the controller with another shielded cable. These two shielded cable were initially double twisted in the vacuum and signal was transmitting out by the electric feedthrough with two pins mounted on the same conflat flange. However, the coupling of these two signals was so strong that controller couldn’t function well, sometimes causing failure of measurement. To solve this problem, these two shielded cables are now totally separated and connected to different feedthroughs mounted on different conflat flanges. The controller output signal can be monitored by an oscilloscope and CPD data is recorded by a computer.

- A potassium dispenser (SAES getter).

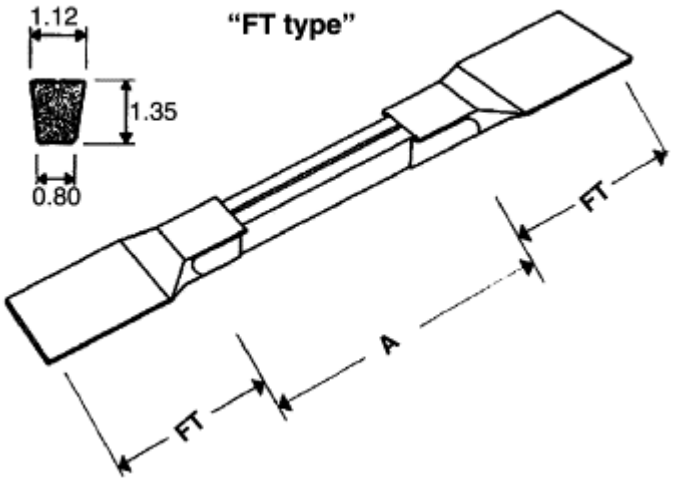

Figure 2-3 Sketch of the SAES getter (potassium dispenser). FT = terminal length = 10mm; A = active length = 17mm.[79]

Sketch of a SAES getter is shown in Figure 2-3. The potassium atoms are evaporated from the slit in the middle of a SAES getter by applying suitable current to an electric feedthrough, where the SAES getter is mounted. A home-made glass tube is used for directional dosing. Note that the SAES getter needs to be degassed before using.

A schematic diagram of the major parts of this UHV system is shown here.

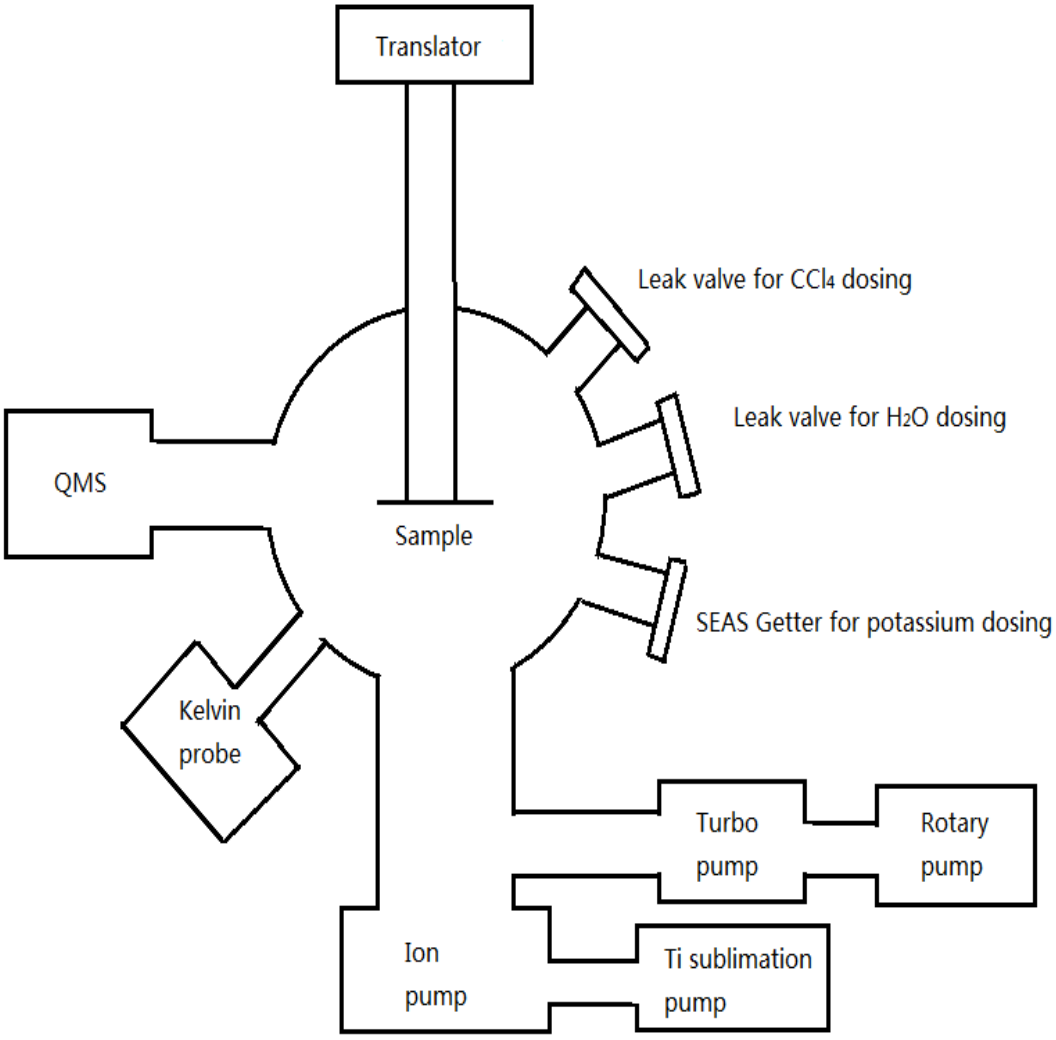

Figure 2-4 Schematic diagram of the UHV system.

2.4.2. Chamber baking

Before the UHV is achieved, the analysis chamber needs to be heated for several hours (sometimes up to days), known as baking, to remove gases (mainly H_2O) adsorbed on the inner wall of the chamber. During baking, the chamber is evenly wrapped by several heating tapes and covered by aluminum foil which can maintain a

baking temperature of about 120℃. The ion pump has a built-in baking system in case the ion pump needs to be baked.

2.4.3. Substrate cleaning

Once the UHV environment is achieved, one can start to perform experiments. The very first thing is to prepare a clean substrate surface. The most common methods to clean a sample surface are heating, chemical treatment and ion sputtering. In our experiment, samples can be cleaned simply by heating. The sample substrate is annealed to 900K for several cycles to remove the residual gases and impurities on the substrate surface.

2.4.4. Sample cooling

The sample can be cooled as low as 90K by introducing liquid nitrogen into one end of the liquid feedthrough, which will lead liquid nitrogen into a reservoir at the back of the sample. The other end of this liquid feedthrough is connected to a mechanical pump, which will constantly evacuate vaporized nitrogen gas out of the liquid feedthrough. A foam container is used to contain liquid nitrogen. The container must be sealed as well as every connected position. Otherwise the capillary of the feedthrough will be jammed by ice which is condensed from water vapor in atmosphere. Ice jamming in the liquid feedthrough will cause cooling failure.

2.4.5. Dosing of gases

In UHV experiments, the Langmuir is the unit to describe the amount of gas dosed into the chamber. One Langmuir corresponds to the exposure of a certain gas in partial pressure 10^{-6} torr for 1 second, i.e. 1L = 10^{-6} torr s. The partial pressure p_0 is measured as the subtraction of initial pressure p_i from final pressure p_f, i.e. $p_0 = p_f - p_i$. The leak valves used in this experiment have a pressure precision in the level of 10^{-9} torr.

Ice film growth is of great importance in our experiment. Because the aim of our project is to determine if CCl_4 adsorption can be enhanced by charged ice surface, uniform solid amorphous ice would be a better choice to get rid of the influence of trapping CCl_4 molecules into a microporous surface. A detailed study of growth of amorphous solid water (ASW) with different deposition conditions has been investigated.[73] It is shown that uniformed ASW will be formed if the deposition temperature is higher than 90K, regardless of deposition angles.

Benefiting from these results, pore-free solid amorphous ice, which is grown from a directional doser at around 100K with a low deposition rate, is grown on a Cu (111) substrate in our experiment.

2.4.6. Dosing of potassium atoms

Potassium atoms are dosed from a SAES getter, which is mounted on the electric feedthrough in order to apply current. The electric feedthrough is connected to the power supply by a circuit which is designed to realize the functions of degassing and

dosing potassium atoms. The following is the schematic diagram.

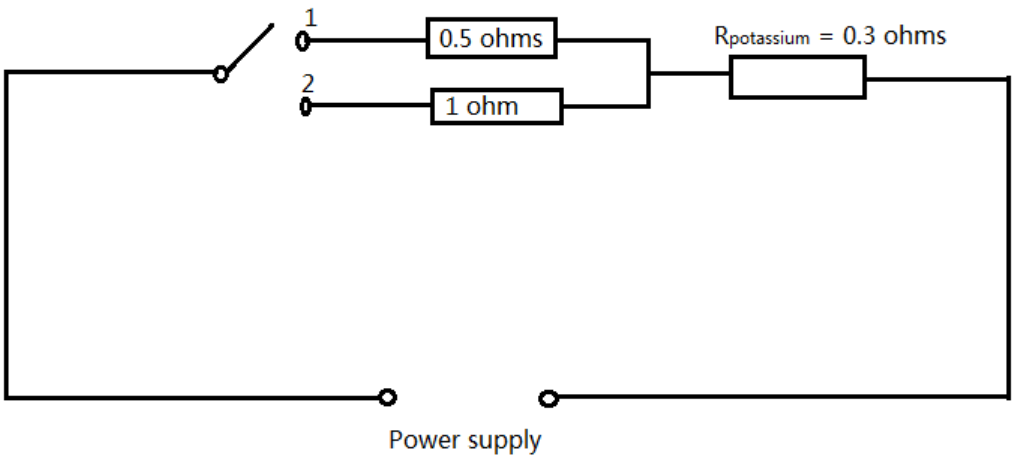

Figure 2-5 Schematic diagram of the control circuit. Position 1 for dosing potassium atoms and 2 for degassing.

Before everyday use, the getter is degassed at about 3A to 4A by putting the switch in position 2 for several hours. Putting the switch in position 1 will increase the current to 6A to evaporate the potassium atoms out of the getter for K deposition.

In our experiment of CCl_4 adsorption on charged ice surfaces, potassium atoms are doped on top of the ice film. It is known that cesium has the lowest ionization energy among the common alkali metals. Thus, it would be easier for cesium to make the ice surface charged and cesium seems to be a better choice. However, cesium atoms can be oxidized very fast even under the ultra-high vacuum at the pressure level of 10^{-9} torr. Balancing the ease of donating electrons and the toughness of preventing from oxidization, potassium is chosen for our experiment.

Chapter 3

Results and discussion

Experimental results for sample calibration (TPD and work function measurements of H_2O) will be illustrated first. Then the results for ice surface charging effect will be shown. At last, CCl_4 adsorption differences on charged and uncharged ice surfaces will be presented.

3.1. Sample calibration

In this section, vacuum back ground, TPD spectra of H_2O, and work function measurements of ice film will be presented respectively.

3.1.1. Vacuum background

Before any experiments were performed, residual background gases in the vacuum chamber were scanned by a quadrupole mass spectrometer (QMS) first at pressure around $5 \times 10^{-10}\ torr$. The scan width and filament current were set up to be 0 – 46 AMU and 1.50 mA respectively.

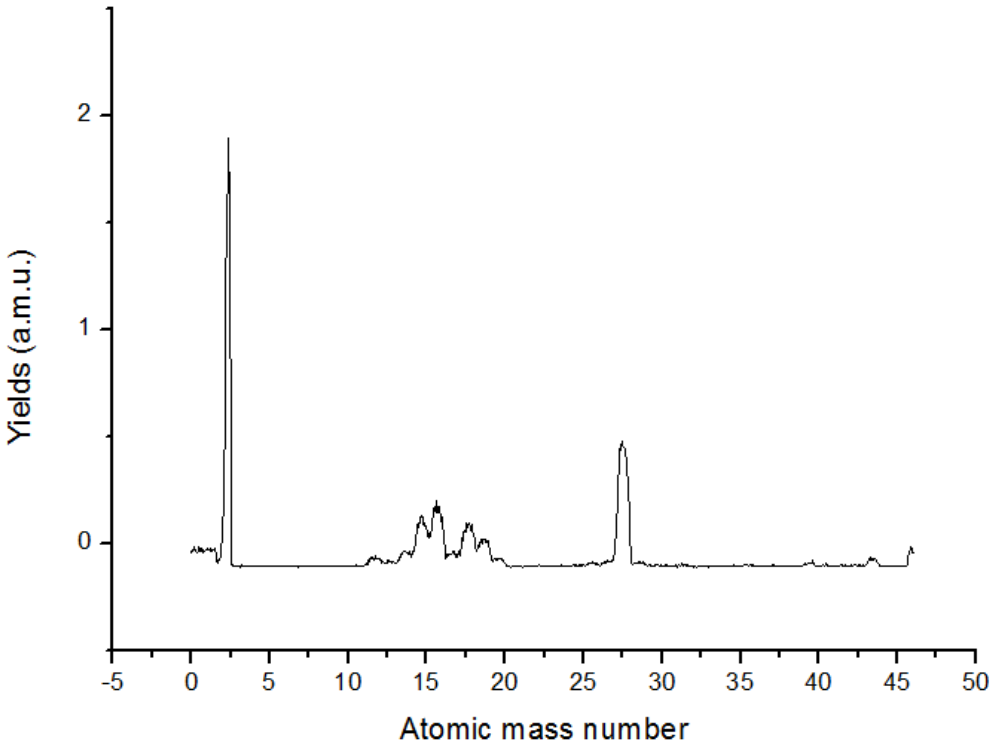

Figure 3-1 QMS scan of background gases with filament 1.5mA.

These peaks depicted by Figure 3-1 are identified to be gases like H_2, O_2, H_2O, N_2, CO_2, and so on, which are considered to be the background noises.

3.1.2. Temperature programmed desorption for H_2O

In order to study the adsorption of CCl_4 on ice surface, H_2O films are always pre-deposited before any other treatments to the sample and multi-layer ice films are used to avoid the influence from the Cu substrate. Calibrations of thickness of the H_2O films will be presented prior to anything else. Temperature programmed desorption (TPD) technique is applied here. First, H_2O molecules in gas phase are introduced into the vacuum chamber and expected to be deposited on substrate at 100 K. Then the heating filament is adjusted to a certain value of current to increase the sample's temperature from 100 K to 200 K at rate about 1 K/s. The H_2O desorption signals are recorded by QMS. Results are shown in Figure 3-2.

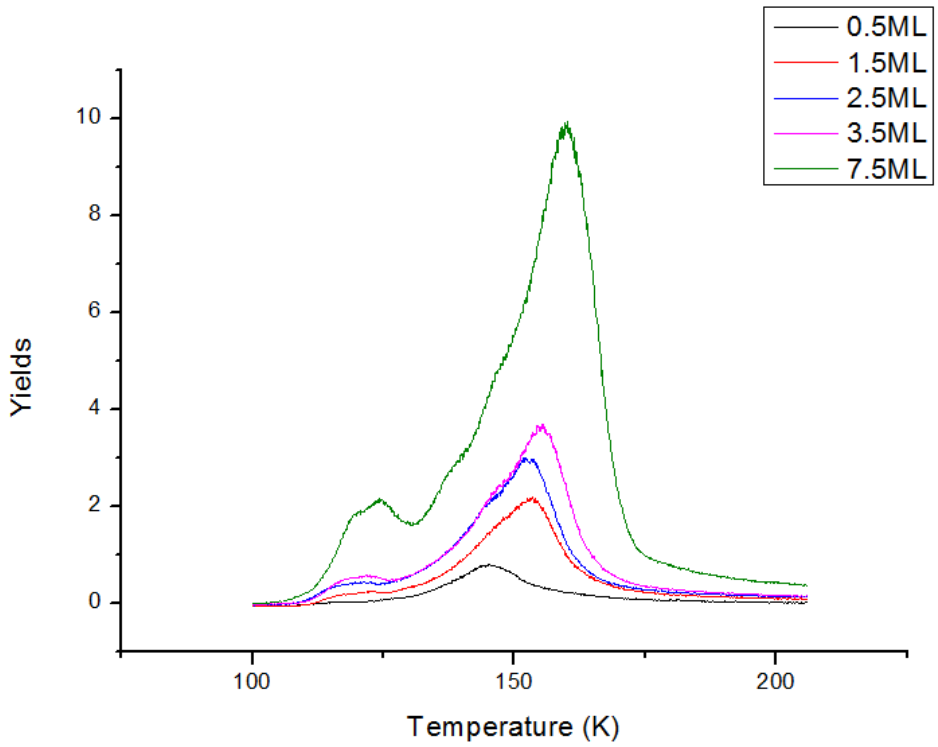

Figure 3-2 TPD spectrum of H_2O with QMS filament 1.0mA.

The scan was fixed at H_2O atomic mass 18 and the filament current was 1.01 mA. As expected, the thicker the water film was, the stronger the H_2O desorption peak would be observed. Considering the filament current was 1.50 mA for background gases scan, the H_2O signal from desorption is overwhelming the background H_2O signal. In fact, ice films with thickness at least 10-ML would be used in the experiments of CCl_4 adsorption. Then, the background gas signal noises should not be a problem.

3.1.3. Work function measurements of ice films

Before any work function measurements, the substrate was annealed to 900 K to clean. The work function of the substrate was measured first as a reference. Then ice films with different thicknesses were deposited on the substrate and the work function changes after the deposition of these ice films were recorded by Kelvin probe as

shown in Table 3-1.

H_2O Coverage (ML)	1	2	7	12	12ML with K deposited
ΔΦ (eV)	-0.28	-0.35	+0.25	+0.18	-2.80

Table 3-1 Work function change of ice films with different thicknesses. For last column, potassium atoms were deposited on top of the ice surface.

It was found that the work function is lowered when the substrate is covered by a one or two monolayer ice film. Since H_2O molecules possess a permanent dipole moment, they are strongly oriented when approaching the Cu substrate.[80] According to Doering and Madey[81], the oxygen will be closer to the substrate for the first H_2O monolayer. Then electrons donated from adsorbed water to substrate will cause the work function decrease.[82] But the work function will eventually increase as the ice film gets thicker because ice is an insulator. Expectedly, deposition of potassium atoms on ice film dramatically reduces its work function.[58]

3.2. Charging ice surface

As it has been discussed in the introduction chapter, the ice surface can get negatively charged once it is deposited by alkali metal atoms, even at very low coverage. For example, deposition of low coverage sodium can dramatically reduce the photoemission threshold.[58] In other words, the work function of ice film will decrease significantly if the alkali atoms are deposited on the ice surface. This is consistent with our experiment results.

In our experiment, potassium atoms were deposited on the ice surface and the work function changes were observed by the Kelvin probe. Interestingly, it was found that the work function changes were strongly dependent on temperature. The sample was prepared as follows. First, the Cu substrate was cleaned by annealing to 900 K and cooled back to 95 K by using liquid N_2. Then the ice film was grown at $5 \times 10^{-9}\ torr$ for 5 minutes (about 15-ML). The measured work function change of this ice film was +2.0 eV before potassium was deposited relative to the work function of substrate. After the potassium was deposited from the getter at 6 A for 2 minutes, the work function change was measured as -0.8eV. That is to say, the work function of the ice film was lowered by 2.8 eV because of potassium deposition. This significant work function decrease can be attributed to the metastable delocalized excess surface electrons donated by potassium atoms undergoing self-ionization on the ice surface. However, this surface charging effect disappeared gradually when the temperature was continuously increased to about 135 K as showed in Figure 3-3.

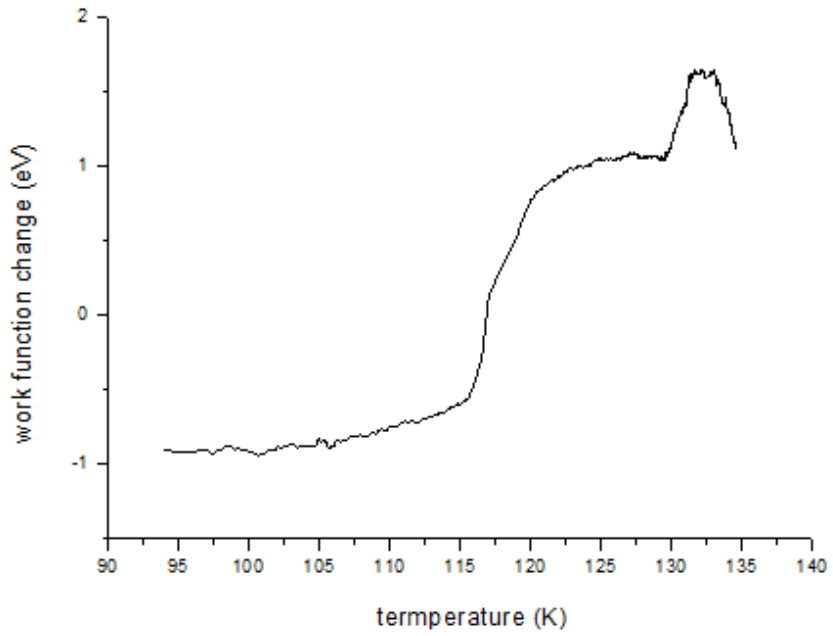

Figure 3-3 Work function change for a 15-ML ice film with freshly deposited potassium, measured as a function of temperature. The current of heating filament was 0.8 A.

Figure 3-3 shows the work function changes verse temperature. The sample is heated by a filament with 0.8 A current. During 5 minutes heating, the work function change is increased slowly below 116 K and then suddenly goes up to a high plateau where a small peak is observed. And the excess surface electrons vanished eventually once the temperature was above 120 K. Thus, the increase of the work function change is due to the loss of excess surface electrons. It is also believed that the peak located at the plateau is caused by the glass transition of ice at about 135 K. Surprisingly, the work function change recovered to -1.0 eV (measured from a multi-meter) as the sample was recooled to 95 K. It seems that this is a reversible process.

However, this reversible phenomenon disappears when the same sample is heated up to 168 K and recooled to 100 K. Figure 3-4 shows the work function change during the heating and Figure 3-5 shows the work function change during the recooling stage.

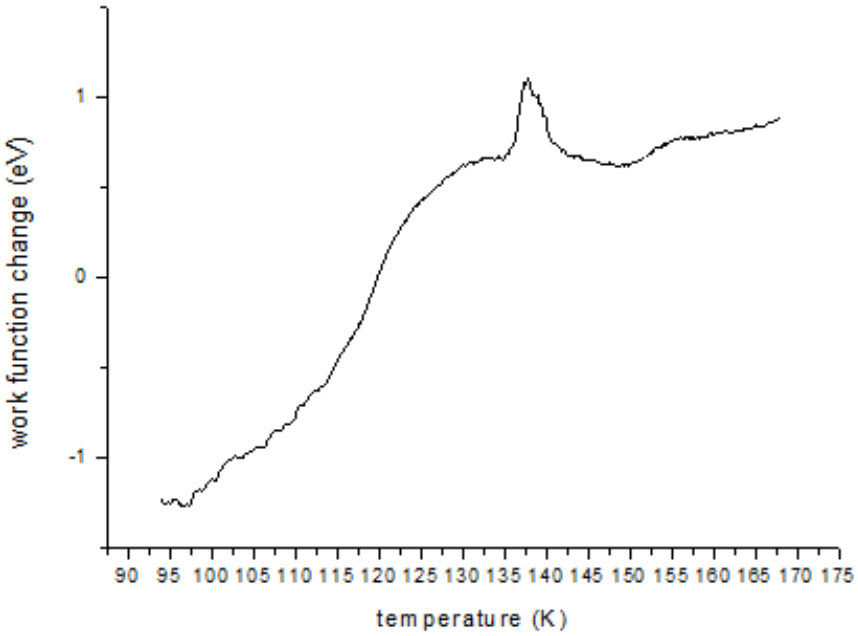

Figure 3-4 Work function change for a 15-ML ice film with freshly deposited potassium, measured as a function of temperature. The current of heating filament was 1.0A.

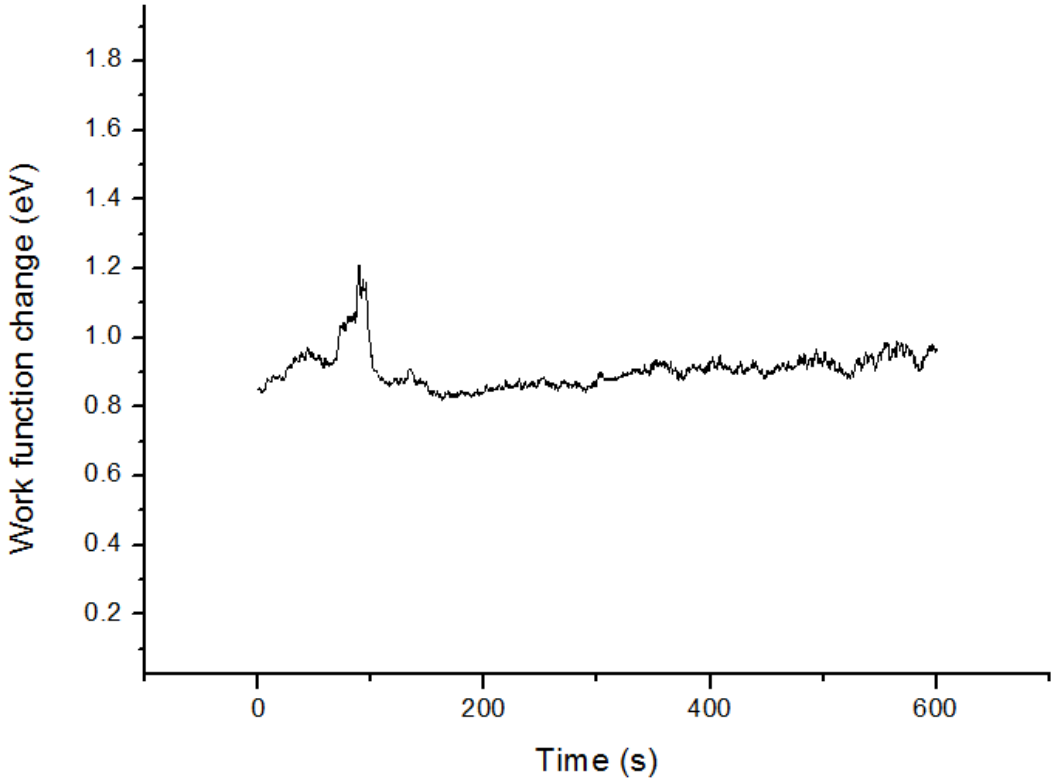

Figure 3-5 Work function change for a 15-ML ice film with freshly deposited potassium after heating to 168 K, measured as a function of cooling time (10 minutes).

In order to get higher temperatures, the current of the heating filament was increased to 1.0 A. According to Figure 3-4, the work function change of the ice film, similar to what is observed in Figure 3-3, increases quickly from -1.0 eV to a plateau and then stabilizes there with a small peak at 137 K. Figure 3-5 shows the work function change during recooling for 10 minutes. Other than a little peak, the work function change remains at +0.9 eV for the whole time instead of going back to -1.0 eV. It is not a reversible process this time.

In the Figure 3-3, the increase of work function can be attributed to the rapid rise of dielectric constant due to the relaxation of stressed amorphous ice when temperature gets up.[45,83] But in the latter case as shown in Figure 3-4, the ice film will experience crystallization when the temperature rises to 168 K. Trapped electrons are probably tunneling back to the Cu(111) substrate and won't come back again even if the substrate is recooled. One should keep in mind that the irreversible work function change only indicates that the trapped electrons will tunnel through the crystalline ice film and reach the metal substrate. This will not happen in PSCs in the atmosphere as there is no metal substrate. In other words, electrons can be trapped in crystalline ice particles in PSCs.

It seems that the density of excess surface electrons is related to temperature. To rule out the potential influence from the ice film deposited from different conditions, the work function change measurements were taken from a 20-ML ice film which was grown at 146 K. K atoms were also deposited on ice at this temperature. Results showed that the work function was only lowered by 0.07eV after deposition of K atoms, which means that almost no excess surface electrons survived from tunneling through the ice film to the Cu(111) substrate.

Conclusively, deposition of potassium on ice film can get the surface charged only below 110K in experiment. Above that, the excess electrons donated by potassium

atoms can't be held by the ice surface and then the surface will be discharged.

3.3. CCl_4 adsorption on ice film

The most important part of this project is to investigate the differences of CCl_4 adsorption on two types of ice film surface, namely charged and uncharged surfaces. From the above sections, a charged ice film can be achieved by deposition of potassium atoms. Also, the temperature of the whole growth process was below 116 K to preserve the excess surface electrons at the ice film from decaying into the metal substrate. Besides, the work function change of the ice surface can be regarded as a tool to study CCl_4 adsorption because work function will be certainly changed if there is any foreign species deposited onto its surface. Results on charged and uncharged ice surfaces will be shown in following sections.

3.3.1. CCl_4 adsorption on ice film without potassium deposition

The sample was prepared as follows. First, the Cu substrate was cleaned by annealing to 900 K and recooled to 104 K. Then an about 30-ML H_2O film was deposited at a pressure of $1 \times 10^{-8}\ torr$ for five minutes. Without deposition of potassium, the sample was heated to 110 K and kept at this temperature. At last, CCl_4 gas was introduced into the vacuum chamber at $5 \times 10^{-8}\ torr$ for 5 minutes when the work function change of the ice surface was recorded. Results are shown in Figure 3-6.

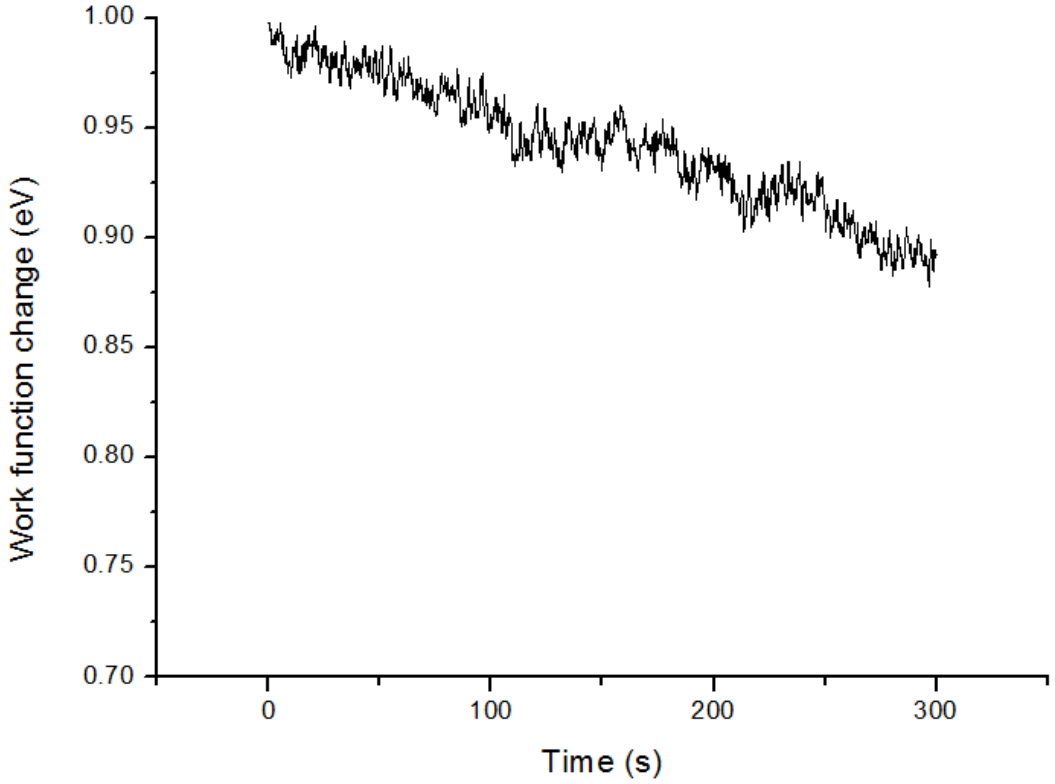

Figure 3-6 Work function change of a 30-ML ice film (no potassium deposition) when CCl_4 gas is introduced into the vacuum chamber at 5×10^{-8} torr for 5 minutes.

During the CCl_4 exposure for 300 s, only a gradual, small decrease of less than 0.1 eV in the surface work function was observed. This can be considered as an insignificant change, indicating that only a small amount of CCl_4 molecules will be adsorbed on uncharged ice surface at 110K for 5 mins at such exposure pressure.

3.3.2. CCl_4 adsorption on potassium-deposited ice film

To compare with the uncharged surface, potassium atoms were deposited to achieve a charged ice surface this time. A 30-ML ice film was grown on the substrate first and then potassium atoms were deposited on top of the ice film at 6 A for 2 minutes. Keeping the temperature at 110 K, CCl_4 was introduced into the vacuum for 150s;

meanwhile the work function change was recorded as shown in Figure 3-7.

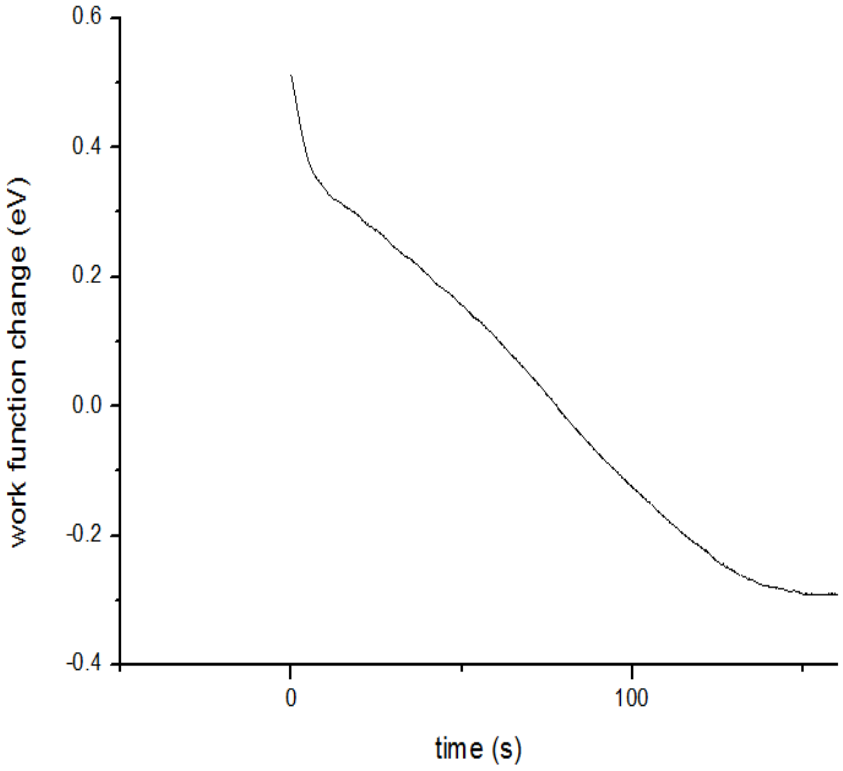

Figure 3-7 Work function change of a 30-ML ice film with freshly deposited potassium when CCl_4 gas is introduced into the vacuum chamber at 5×10^{-8} torr for 150s.

For this charged ice surface, the work function change is dramatically different from what was observed on the uncharged ice surface. Exposure of CCl_4 will cause a significant decrease of 0.8 eV in work function change.

The decrease of the work function can be attributed to the adsorption of CCl_4 on ice. At 110 K, only a small amount of CCl_4 molecules is adsorbed on uncharged ice film as it is shown in last section. But the charged ice surface exhibits very different properties from a normal ice surface. Generally speaking, the charged surface will create an electric field which can polarize gas molecules and then adsorb them by electrostatic binding.[7] Once the gas molecules have adsorbed on the surface, the work function change of such a surface will be observed.

3.4. Temperature dependence of CCl_4 adsorption on potassium-deposited ice surface

It has been shown that surface excess electrons are very sensitive to temperature. They vanish quickly once the temperature is higher than 116 K. From the different results of experiments performed on charged and uncharged ice surfaces, CCl_4 molecules are believed to be captured easily by ice surfaces with excess surface electrons. To further confirm the critical role of excess surface electrons in CCl_4 adsorption, work function change measurements were carried out on a potassium-deposited ice film at high temperature (145K) and low temperature (100K) respectively.

3.4.1. High temperature adsorption measurements

A 15-ML ice film was prepared with deposition of K atoms at 95 K. The sample temperature was then increased and kept at 145 K. At last, the CCl_4 gas was introduced into the chamber immediately at an exposure of 5×10^{-8} torr for 300s. The work function change is recorded as shown in figure 3-9.

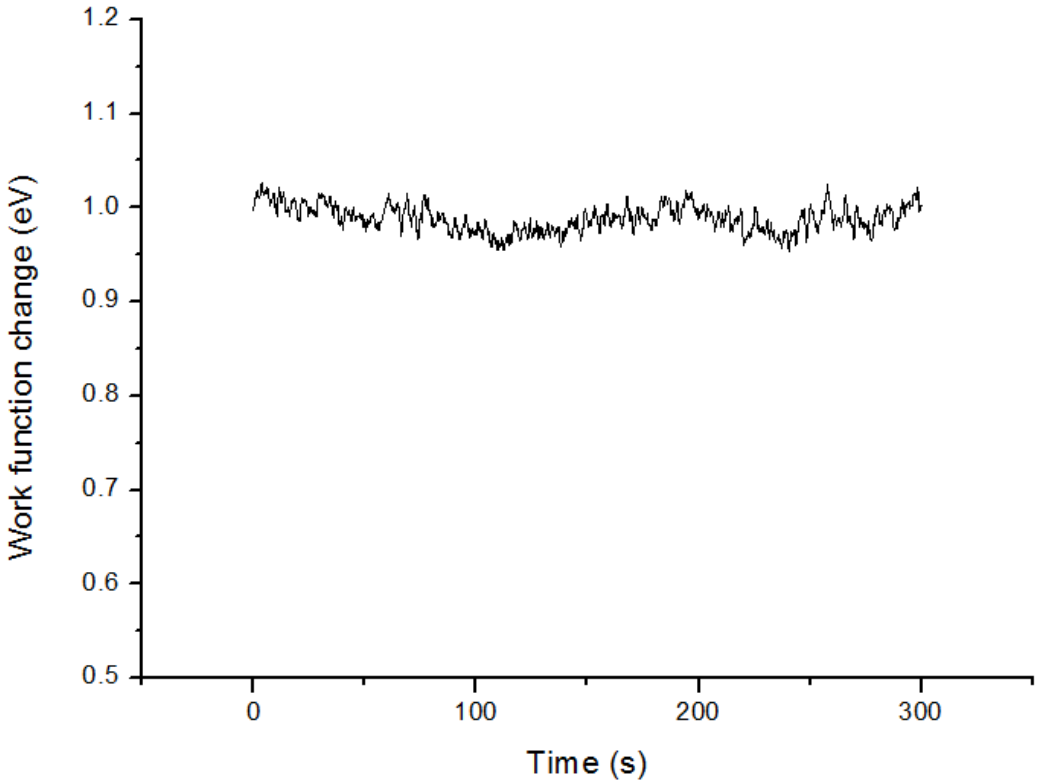

Figure 3-8 Work function change measurement of a potassium-deposited ice film during CCl_4 exposure at 5×10^{-8} torr for 5 minutes at 145K.

As shown in Figure 3-9, the work function stays almost the same throughout the 5 minutes of CCl_4 exposure. No change in work function means that CCl_4 molecules cannot be adsorbed on this potassium-deposited ice film.

It has been determined that excess surface electrons will vanish once the temperature is higher than 120 K. This experiment was done at 145 K so that no excess electrons survived. It should not be surprising to observe that adsorption of CCl_4 doesn't happen in this case.

3.4.2. Low temperature adsorption measurements

In order to compare with the characteristics of high temperature CCl_4 adsorption, a CCl_4 adsorption experiment at low at temperature (100 K) was performed. One would argue whether CCl_4 molecules can be adsorbed on both charged and uncharged ice surfaces at such low temperature. To estimate the nature of condensation of CCl_4 on ice surfaces at low temperature, the work function change of an uncharged ice film during CCl_4 exposure at 100 K is presented first in table 3-2 as a reference.

CCl_4 exposure time (min)	Work function change (eV)
2	-0.022
3	-0.042
4	-0.032
5	-0.032
6	-0.028
8	-0.031
10	-0.022

Table 3-2 Work function change of the ice film during CCl_4 exposure for 10 minutes.

The exposure pressure of CCl_4 was $5 \times 10^{-8}\, torr$ for the first 2 minutes and increased to $1 \times 10^{-7}\, torr$ for the following 8 minutes. As shown in Table 3-2, very small work function changes are detected during the 10 minutes of CCl_4 exposure. That is to say, just a small amount of CCl_4 molecules would be adsorbed on normal uncharged ices surface at 100 K at this exposure time and pressure.

Then, a 12-ML ice film was prepared with freshly deposited K atoms at 100 K. Keeping the temperature at about 100 K, the CCl_4 gas was introduced into the chamber immediately for 600s. The work function change is recorded as shown in Figure 3-10.

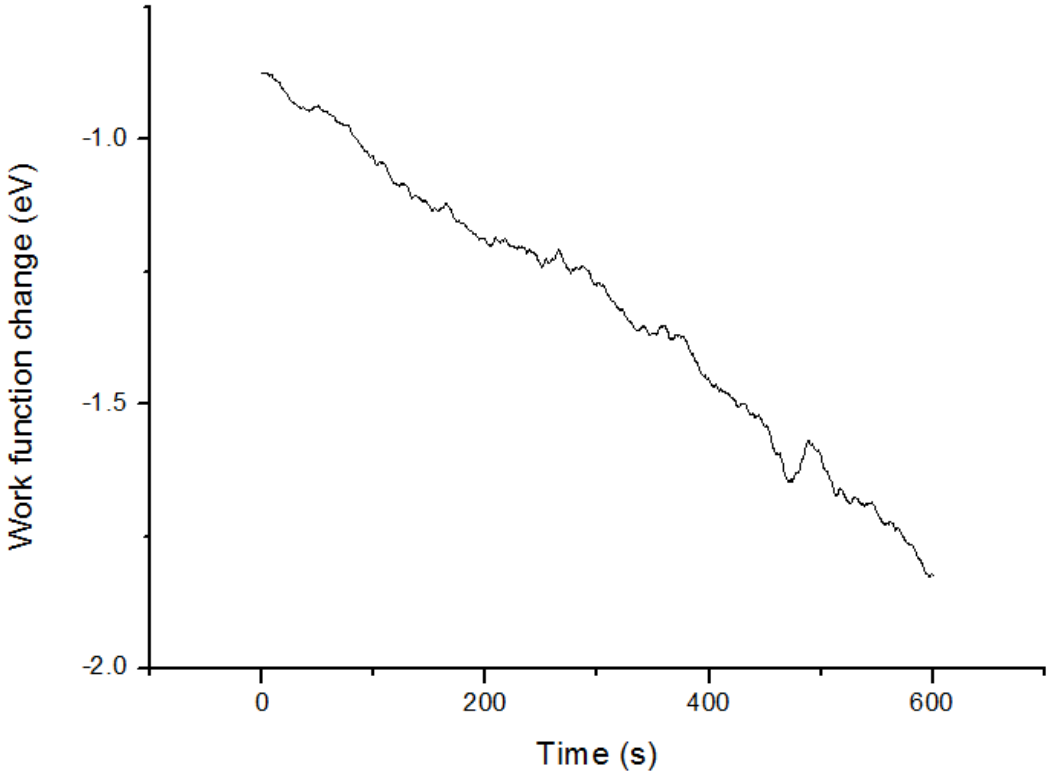

Figure 3-9 Work function change measurement of a potassium-deposited ice film during CCl_4 exposure for 10 minutes at 100K.

During CCl_4 exposure at 100K, the work function was decreased by 1 eV, which revealed the significant adsorption of CCl_4 due to high density of excess surface electrons at low temperature. Because the condensation of CCl_4 has been ruled out, this further confirms that charged ice surfaces exhibit very different properties from uncharged ice surfaces.

Above all, it is found that CCl_4 molecules can be obviously adsorbed on charged ice surfaces under certain conditions and barely adsorbed by uncharged ice surface above 100 K. In addition, the adsorption of CCl_4 on charged ice surfaces is dependent on the density of excess surface electrons, which are further dependent on temperature.

Chapter 4

Conclusion

In this study, ice surface charging effect was explored first and it is found that deposition of potassium atoms can significantly reduce the work function of ice films. This effect is attributed to the formation of metastable delocalized excess surface electrons which are donated by potassium atoms undergoing self-ionization on ice. However, the density of excess surface electrons is determined to be a function of temperature. Work function change measurements show that excess surface electrons can only survive below 116 K and they will totally vanish above 120 K. Therefore, the potassium-deposited ice surface can be regarded as charged ice surface only at very low temperature.

Then CCl_4 adsorption differences on charged and uncharged ice surface were investigated in this study. Experimental results show almost no adsorption of CCl_4 on uncharged ice surface. But CCl_4 molecules can be effectively adsorbed on charged ice surface. It is believed that CCl_4 adsorption on charged ice surfaces is due to electrostatic effects induced by the high density of excess surface electrons. The critical role of excess surface electrons in CCl_4 adsorption is further confirmed by conducting experiments at different temperatures. Results are quite consistent with the temperature dependence of density of excess surface electrons which we found earlier.

The characteristic of CCl_4 adsorption on charged ice surface can be applied to the CRE ozone depletion model which is originally proposed by Dr. Lu and co-workers. Our results totally support that CFCs are very likely to be adsorbed on ice particle

surfaces in PSCs where cosmic ray ionization will get these small ice particles charged. Once CFCs adsorbed on ice surfaces, the DET mechanism is believed to take place effectively as described in the CRE model. Then the resultant chlorine atoms will be generated after a series of reactions to destroy ozone.

References

1 Q. B. Lu, "Cosmic-ray-driven electron-induced reactions of halogenated molecules adsorbed on ice surfaces: Implications for atmospheric ozone depletion and global climate change," Phys Rep **487** (5), 141-167 (2010).

2 S. B. Maclane E. W. Müller, and J. A. Panitz, "The Atom-Probe Field Ion Microscope," Rev. Sci. Instrum. **39** (1), 83-86 (1968).

3 T. T. Tsong and E. W. Muller, "Field Adsorption of Inert-Gas Atoms," J Chem Phys **55** (6), 2884-& (1971).

4 T. T. Tsong, "The Kinetics of Field Adsorption," Surf Sci **140** (2), 377-392 (1984).

5 D. Tomanek, H. J. Kreuzer, and J. H. Block, "Tight-Binding Approach to Field Desorption - N2 on Fe(111)," Surf Sci **157** (1), L315-L322 (1985).

6 K. Nath, H. J. Kreuzer, and A. B. Anderson, "Field Adsorption of Rare-Gases," Surf Sci **176** (1-2), 261-283 (1986).

7 N. Shamir, J. G. Mihaychuk, H. M. van Driel, and H. J. Kreuzer, "Universal mechanism for gas adsorption and electron trapping on oxidized silicon," Phys Rev Lett **82** (2), 359-361 (1999).

8 M. J. Molina and F. S. Rowland, "Stratospheric Sink for Chlorofluoromethanes - Chlorine Atomic-Catalysed Destruction of Ozone," Nature **249** (5460), 810-812 (1974).

9 P. J. Crutzen, "Ozone Production Rates in an Oxygen-Hydrogen-Nitrogen Oxide Atmosphere," J Geophys Res **76** (30), 7311-& (1971).

10 J. C. Farman, B. G. Gardiner, and J. D. Shanklin, "Large Losses of Total Ozone in Antarctica Reveal Seasonal Clox/Nox Interaction," Nature **315**

(6016), 207-210 (1985).

11 S. Solomon, "Progress Towards a Quantitative Understanding of Antarctic Ozone Depletion," Nature **347** (6291), 347-354 (1990).

12 O. B. Toon and R. P. Turco, "Polar Stratospheric Clouds and Ozone Depletion," Sci Am **264** (6), 68-74 (1991).

13 L. Sanche, "Interactions of Low-Energy Electrons with Atomic and Molecular-Solids," Scanning Microscopy **9** (3), 619-656 (1995).

14 G. J. Schulz, "Resonances in Electron-Impact on Diatomic-Molecules," Rev Mod Phys **45** (3), 423-486 (1973).

15 A. Chutjian, A. Garscadden, and J. M. Wadehra, "Electron attachment to molecules at low electron energies," Phys Rep **264** (6), 393-470 (1996).

16 R. A. Marcus, "Electron-Transfer Reactions in Chemistry - Theory and Experiment," Rev Mod Phys **65** (3), 599-610 (1993).

17 A.M. Kuznetsov (ed), *Charge Transfer in Physics, Chemistry and Biology*. (OPA, Amsterdam B.V., 1995).

18 S. Larsson, "Electron-Transfer in Chemical and Biological-Systems - Orbital Rules for Non-Adiabatic Transfer," J Am Chem Soc **103** (14), 4034-4040 (1981).

19 R.E. Johnson (ed), *Energetic Charge-Particles Interactions with Atmospheres and Surfaces, in: Physics and Chemistry in Space Planetology*. (Springer-Verlag, Berlin, 1990).

20 B. M. Nestmann, S. V. K. Kumar, and S. D. Peyerimhoff, "Contribution of Feshbach resonance to the 1.3-eV dissociative-electron-attachment cross section of ozone," Phys Rev A **71** (1) (2005).

21 E. Illenberger, H. U. Scheunemann, and H. Baumgartel, "Fragmentation of Halomethanes under Impact with Low-Energy (0-10ev) Monochromatic Electrons," Ber Bunsen Phys Chem **82** (11), 1154-1158 (1978).

22 E. Illenberger, H. U. Scheunemann, and H. Baumgartel, "Negative-Ion Formation in Cf2cl2,Cf3cl and Cfcl3 Following Low-Energy (0-10ev) Impact

with near Monoenergetic Electrons," Chem Phys **37** (1), 21-31 (1979).

23 S. D. Peyerimhoff and R. J. Buenker, "Potential Curves for Dissociative Electron-Attachment of Cfcl3," Chem Phys Lett **65** (3), 434-439 (1979).

24 M. Lewerenz, B. Nestmann, P. J. Bruna, and S. D. Peyerimhoff, "The Electronic-Spectrum, Photodecomposition and Dissociative Electron-Attachment of Cf2cl2 - an Abinitio Configuration-Interaction Study," Theochem-J Mol Struc **24** (3-4), 329-342 (1985).

25 N.G. Adams D. Smith, "Visual acuity following binocular deprivation in the cat," Top. Curr. Chem. **183** (1), 11 (1980).

26 D.G. Torr (ed), *The Photochemistry of Atmospheres*. (Academic Press, Orlando, 1985).

27 Q. B. Lu and T. E. Madey, "Giant enhancement of electron-induced dissociation of chlorofluorocarbons coadsorbed with water or ammonia ices: Implications for atmospheric ozone depletion," J Chem Phys **111** (7), 2861-2864 (1999).

28 Q. B. Lu and T. E. Madey, "Negative-ion enhancements in electron-stimulated desorption of CF2Cl2 coadsorbed with nonpolar and polar gases on Ru(0001)," Phys Rev Lett **82** (20), 4122-4125 (1999).

29 Q. B. Lu and T. E. Madey, "Mechanism for giant Cl- and F- enhancements in electron-induced dissociation of CF2Cl2 coadsorbed with water or ammonia ices," Surf Sci **451** (1-3), 238-243 (2000).

30 Q. B. Lu and T. E. Madey, "Factors influencing Cl- and F- enhancements in electron-stimulated desorption of CF2Cl2 coadsorbed with other gases," J Phys Chem B **105** (14), 2779-2784 (2001).

31 C. Silva, P. K. Walhout, K. Yokoyama, and P. F. Barbara, "Femtosecond solvation dynamics of the hydrated electron," Phys Rev Lett **80** (5), 1086-1089 (1998).

32 Q. B. Lu and L. Sanche, "Effects of cosmic rays on atmospheric chlorofluorocarbon dissociation and ozone depletion," Phys Rev Lett **87** (7)

(2001).

33 Q. B. Lu, "Correlation between Cosmic Rays and Ozone Depletion," Phys Rev Lett **102** (11) (2009).

34 Q. B. Lu and L. Sanche, "Enhanced dissociative electron attachment to CF2Cl2 by transfer of electrons in precursors to the solvated state in water and ammonia ice," Phys Rev B **63** (15) (2001).

35 Q. B. Lu and L. Sanche, "Large enhancement in dissociative electron attachment to HCl adsorbed on H2O ice via transfer of presolvated electrons," J Chem Phys **115** (13), 5711-5713 (2001).

36 Q. B. Lu and L. Sanche, "Condensed-phase effects on absolute cross sections for dissociative electron attachment to CFCs and HCFCs adsorbed on Kr," J Chem Phys **119** (5), 2658-2662 (2003); Q. B. Lu and L. Sanche, "Enhancements in dissociative electron attachment to CF4, chlorofluorocarbons and hydrochlorofluorocarbons adsorbed on H2O ice," J Chem Phys **120** (5), 2434-2438 (2004).

37 C. R. Wang and Q. B. Lu, "Real-time observation of a molecular reaction mechanism of aqueous 5-Halo-2 '-deoxyuridines under UV/ionizing radiation," Angewandte Chemie-International Edition **46** (33), 6316-6320 (2007).

38 S. Ryu, J. Chang, H. Kwon, and S. K. Kim, "Dynamics of solvated electron transfer in thin ice film leading to a large enhancement in photodissociation of CFCl3," J Am Chem Soc **128** (11), 3500-3501 (2006).

39 C. R. Wang, T. Luo, and Q. B. Lu, "On the lifetimes and physical nature of incompletely relaxed electrons in liquid water," Phys Chem Chem Phys **10** (30), 4463-4470 (2008).

40 F. Baletto, C. Cavazzoni, and S. Scandolo, "Surface trapped excess electrons on ice," Phys Rev Lett **95** (17) (2005).

41 M. Bertin, M. Mever, J. Stahler, C. Gahl, M. Wolf, and U. Bovensiepen, "Reactivity of water-electron complexes on crystalline ice surfaces," Faraday

Discuss **141**, 293-307 (2009).

42 K. L. Foster, M. A. Tolbert, and S. M. George, "Interaction of HCl with ice: Investigation of the predicted trihydrate, hexahydrate, and monolayer regimes," J Phys Chem A **101** (27), 4979-4986 (1997).

43 M. J. Isakson and G. O. Sitz, "Adsorption and desorption of HCl on ice," J Phys Chem A **103** (13), 2044-2049 (1999).

44 V. Sadtchenko, C. F. Giese, and W. R. Gentry, "Interaction of hydrogen chloride with thin ice films: The effect of ice morphology and evidence for unique surface species on crystalline vapor-deposited ice," J Phys Chem B **104** (40), 9421-9429 (2000).

45 Q. B. Lu, T. E. Madey, L. Parenteau, F. Weik, and L. Sanche, "Structural and temperature effects on Cl- yields in electron-induced dissociation of CF2Cl2 adsorbed on water ice," Chem Phys Lett **342** (1-2), 1-6 (2001).

46 D. Emin, "Small Polarons," Phys Today **35** (6), 34-40 (1982).

47 F. S. Dainton, "Electrons in Condensed Media," Berich Bunsen Gesell **75** (7), 608-& (1971).

48 J. Staehler, C. Gahl, and M. Wolf, "Dynamics and Reactivity of Trapped Electrons on Supported Ice Crystallites," Accounts Chem Res **45** (1), 131-138 (2012).

49 J. P. Coad, H. E. Bishop, and J. C. Riviere, "Electron-Beam Assisted Adsorption on Si(111) Surface," Surf Sci **21** (2), 253-& (1970).

50 H. Ibach, K. Horn, R. Dorn, and H. Luth, "Adsorption of Oxygen on Silicon (111) Surfaces .1.," Surf Sci **38** (2), 433-454 (1973).

51 B. A. Joyce and J. H. Neave, "Electron Beam-Adsorbate Interactions on Silicon Surfaces," Surf Sci **34** (2), 401-419 (1973).

52 J. L. Vignes, P. Denjean, J. Lehericy, and J. P. Langeron, "Cleanliness and Pollution of Si(111) and Si(100) Surfaces Studied by Aes," Surf Sci **168** (1-3), 59-67 (1986).

53 J. Chiebek K. T. Kohlmann-von Platen, M. Weiss, K. Reimer, H. Oertel, and

W. H. Brunger, "Resolution limits in electron-beam induced tungsten deposition," J. Vac. Sci. Technol. B **11** (6), 2219-2223 (1993).

54 K I Schiffmann, "Investigation of fabrication parameters for the electron-beam-induced deposition of contamination tips used in atomic force microscopy," Nanotechnology **4** (3), 163-169 (1993).

55 H. T. Liu and Z. Wu, "The Role of Secondary Electrons in Electron-Assisted Adsorption Process," Surf Sci **290** (1-2), L685-L687 (1993).

56 N. Silvis-Cividjian, C. W. Hagen, L. H. A. Leunissen, and P. Kruit, "The role of secondary electrons in electron-beam-induced-deposition spatial resolution," Microelectron Eng **61-2**, 693-699 (2002).

57 T. E. Madey and J. T. Yates, "Electron-Stimulated Desorption and Work Function Studies of Clean and Cesiated (110) Gaas," J Vac Sci Technol **8** (1), 39-& (1971).

58 T. Vondrak, S. R. Meech, and J. M. C. Plane, "Photoelectric emission from the alkali metal doped vacuum-ice interface," J Chem Phys **130** (5) (2009).

59 W. R. Haag and C. C. D. Yao, "Rate Constants for Reaction of Hydroxyl Radicals with Several Drinking-Water Contaminants," Environ Sci Technol **26** (5), 1005-1013 (1992).

60 W. Mabey and T. Mill, "Critical-Review of Hydrolysis of Organic-Compounds in Water under Environmental-Conditions," J Phys Chem Ref Data **7** (2), 383-415 (1978).

61 C. S. Criddle and P. L. Mccarty, "Electrolytic Model System for Reductive Dehalogenation in Aqueous Environments," Environ Sci Technol **25** (5), 973-978 (1991).

62 I. Hua and M. R. Hoffmann, "Kinetics and mechanism of the sonolytic degradation of CCl4: Intermediates and byproducts," Environ Sci Technol **30** (3), 864-871 (1996).

63 F. Sabin, T. Turk, and A. Vogler, "Photooxidation of Organic-Compounds in the Presence of Titanium-Dioxide - Determination of the Efficiency," J

Photoch Photobio A **63** (1), 99-106 (1992).

64 H. U. Scheunemann, E. Illenberger, and H. Baumgartel, "Dissociative Electron-Attachment to Ccl4, Chcl3, Ch2cl2 and Ch3cl," Ber Bunsen Phys Chem **84** (6), 580-585 (1980).

65 C. R. Wang, K. Drew, T. Luo, M. J. Lu, and Q. B. Lu, "Resonant dissociative electron transfer of the presolvated electron to CCl(4) in liquid: Direct observation and lifetime of the CCl(4)*(-) transition state," J Chem Phys **128** (4) (2008).

66 R. A. Popple, C. D. Finch, K. A. Smith, and F. B. Dunning, "Dissociative electron attachment to CCl4: Lifetime of the CCl4-* intermediate," J Chem Phys **104** (21), 8485-8489 (1996).

67 N. Shamir, J. G. Mihaychuk, and H. M. van Driel, "Trapping and detrapping of electrons photoinjected from silicon to ultrathin SiO2 overlayers. I. In vacuum and in the presence of ambient oxygen," J Appl Phys **88** (2), 896-908 (2000).

68 N. Shamir and H. M. van Driel, "Trapping and detrapping of electrons photoinjected from silicon to ultrathin SiO2 overlayers. II. In He, Ar, H-2, N-2, CO, and N2O," J Appl Phys **88** (2), 909-917 (2000).

69 T. Vondrak, J. M. C. Plane, and S. R. Meech, "Photoemission from sodium on ice: A mechanism for positive and negative charge coexistence in the mesosphere," J Phys Chem B **110** (9), 3860-3863 (2006).

70 T. Vondrak, J. M. C. Plane, and S. R. Meech, "Influence of submonolayer sodium adsorption on the photoemission of the Cu(111)/water ice surface," J Chem Phys **125** (22) (2006).

71 Y. Horowitz and M. Asscher, "Low energy charged particles interacting with amorphous solid water layers," J Chem Phys **136** (13) (2012).

72 D. and Kauzmann Eizenberg, W (ed), *The structure and Properties of water*. (Oxford University Press, New York, 1969).

73 K. P. Stevenson, G. A. Kimmel, Z. Dohnalek, R. S. Smith, and B. D. Kay,

"Controlling the morphology of amorphous solid water," Science **283** (5407), 1505-1507 (1999).

74 V. Sadtchenko, K. Knutsen, C. F. Giese, and W. R. Gentry, "Interactions of CCl4 with thin D2O amorphous ice films, part I: A nanoscale probe of ice morphology," J Phys Chem B **104** (11), 2511-2521 (2000).

75 R. S. Smith, C. Huang, E. K. L. Wong, and B. D. Kay, "The molecular volcano: Abrupt CCl4 desorption driven by the crystallization of amorphous solid water," Phys Rev Lett **79** (5), 909-912 (1997).

76 V.G. Lifshits K. Oura, A. A. Saranin, A. V. Zotov, M. Katayama (ed), *Surface Science - An Introduction*. (Springer-Verlag, 2003).

77 P.A. Redhead, "Thermal Desorption of Gases," Vacuum **12**, 203-211 (1962).

78 Masaki Takihara, "Kelvin Probe Force Microscopy (KFM)", (2007), Vol. 2012.

79 J. P. Temirov, N. V. Chigarev, O. I. Matveev, N. Omenetto, B. W. Smith, and J. D. Winefordner, "A resonance ionization imaging detector based on cesium atomic vapor," Spectrochim Acta B **59** (5), 677-687 (2004).

80 D. E. Grider, K. Bange, and J. K. Sass, "Work Function Changes Due to the Co-Adsorption of Water with Oxygen and Bromine on Cu(110)," J Electrochem Soc **130** (1), 246-248 (1983).

81 D. L. Doering and T. E. Madey, "The Adsorption of Water on Clean and Oxygen-Dosed Ru(001)," Surf Sci **123** (2-3), 305-337 (1982).

82 P. A. Thiel and T. E. Madey, "The Interaction of Water with Solid-Surfaces - Fundamental-Aspects," Surf Sci Rep **7** (6-8), 211-385 (1987).

83 A. A. Tsekouras, M. J. Iedema, and J. P. Cowin, "Amorphous Water-Ice Relaxations Measured with Soft-Landed Ions," Phys Rev Lett **80** (26), 5798-5801 (1998).